

<https://doi.org/10.1590/2318-0331.282320220088>

Discretization approach for large-scale sediment modeling: calibration strategies based on hydro-sediment variability at a range of spatial scales

Abordagem de discretização para modelagem de sedimentos em grande escala: estratégias de calibração baseadas na variabilidade hidrossedimentológica em múltiplas escalas espaciais

Renata Barão Rossoni¹  & Fernando Mainardi Fan¹ 

¹Universidade Federal do Rio Grande do Sul, Porto Alegre, RS, Brasil

E-mails: renata.rossoni@ufrgs.br (RBR), fernando.fan@ufrgs.br (FMF)

Received: November 21, 2022 – Revised: December 09, 2022 – Accepted: December 12, 2022

ABSTRACT

The lack of observed data and calibration strategies, scale variability, and difficulties in representing heterogeneity of sediment-processes contribute to the usual challenges in achieving satisfactory results in hydro-sedimentological modeling, particularly when using the MUSLE equation for large-scale applications. As a consequence, we investigated five major topics: (1) a sediment-process-based parameterization technique (Hydro-sedimentological Response Unit map - HRUSed); (2) the quality of hydrological modeling with different process-focused parameterizations; (3) a calibration strategy based on the sediment discretization approach for hydro-sedimentological modeling; (4) the use of suspended sediment concentration (SSC) versus suspended sediment discharge (SSD) data for calibration; and (5) trade-offs between increasing the spatial resolution of a large-scale model and using the proposed HRUSed discretization. The current study demonstrated (1) the HRUSed map for South America and (2) a similar performance of large-scale hydrological modeling using a hydrological or hydro-sedimentological discretization approach. (3) The HRUSed discretization approach produced better hydro-sedimentological modeling results. (4) We improved the model's performance for HRUSed (SSC and SSD results) and for HRU (Hydrological Response Unit map) only for SSD results. (5) Only more detailed spatial discretization has failed to improve process representation. However, increased spatial discretization with a process-parameterization approach focused on hydro-sedimentological dynamics improved model performance.

Keywords: MGB-SED; MUSLE; Modeling; Sediment; Hydrossedimentology.

RESUMO

A falta de dados observados e estratégias de calibração, a variabilidade de escalas e as dificuldades em representar a heterogeneidade dos processos de erosão e sedimentação contribuem para os desafios usuais na obtenção de resultados satisfatórios na modelagem hidrossedimentológica, particularmente quando se usa a equação MUSLE para aplicações em larga escala. Como consequência, investigamos cinco tópicos principais: (1) uma técnica de parametrização baseada em processos de produção de sedimentos (mapa da unidade de resposta hidrossedimentológica - HRUSed); (2) a qualidade da modelagem hidrológica com diferentes parametrizações focadas nos processos; (3) uma estratégia de calibração baseada na abordagem de discretização focada em sedimentos para modelagem hidrossedimentológica; (4) o uso de dados de concentração de sedimentos em suspensão (CSS) versus descarga de sedimentos em suspensão (DSS) para calibração; e (5) trade-offs entre aumentar a resolução espacial de um modelo de grande escala e usar a discretização HRUSed proposta. O presente estudo demonstrou: (1) o mapa HRUSed para a América do Sul e (2) um desempenho semelhante de modelagem hidrológica em larga escala usando uma abordagem de discretização hidrológica ou hidrossedimentológica; (3) A abordagem de discretização HRUSed produziu melhores resultados de modelagem hidrossedimentológica; (4) Melhoramos o desempenho do modelo para HRUSed (resultados CSS e DSS) e para HRU (mapa de unidades de resposta hidrológica) apenas para resultados de DSS; e (5) adotar apenas uma discretização espacial mais detalhada falhou em melhorar a representação dos processos. No entanto, o aumento da discretização espacial com uma abordagem de parametrização de processos focada na dinâmica hidrossedimentológica melhorou o desempenho do modelo.

Palavras-chave: MGB-SED; MUSLE; Modelagem; Sedimento; Hidrossedimentologia.



INTRODUCTION

Natural movements along the watershed include soil detachment, transportation, and deposition. They are necessary for transporting nutrients, providing natural habitats (Koiter et al., 2013), and altering landscape geomorphology (Dean et al., 2016). Human activities, on the other hand, have the potential to alter hydro-sedimentological processes, increasing the need to understand and quantify current and long-term changes. Mathematical modeling is a useful tool for applying sediment measured data to various scenarios and estimating these changes over time. It aids in understanding sediment dynamics (Rahmati et al., 2017; Vigiak et al., 2017; Wang et al., 2018; Wesselman et al., 2019), the impact of land use (Blainski et al., 2017; Silva et al., 2016) and climate change, reservoir sedimentation (Tadesse & Dai, 2019) and management strategies (Zarzuelo et al., 2019), reservoir capacity loss forecasting (Ahbari et al., 2018), and understanding sediment transport in ecosystems (Wang et al., 2018).

To represent heterogeneity in large-scale modeling, a common approach in hydro-sedimentological modeling combines a conceptual hydrological model with an empirical model from the USLE (Universal Soil Loss Equation) family. Conceptual models represent mechanisms as a series of storage, inferring hydrological and hydro-sedimentological processes without providing specific details (Merritt et al., 2003). It means they have a physical foundation, but we still need to calibrate them. These models were created in response to the need to comprehend basic hydrologic processes over large areas (Arnold et al., 1998). The MUSLE (Modified Universal Soil Loss Equation) (Williams, 1975) aids in the understanding of intra-annual variation in hydro-sediment systems as well as event-based loss estimation. It operates on a shorter time scale than the original USLE and estimates event-based sediment yield using runoff and peak flow (Benavidez et al., 2018; Sadeghi et al., 2014). The MUSLE is used in sediment models such as SWAT (Arnold et al., 1998), WASA-SED (Mueller et al., 2010) and MGB-SED (Buarque, 2015; Fagundes et al., 2019, 2020a, 2020b).

These models typically represent their area, processes, and parameters as distributed models, with the spatial and temporal scales important for representing the processes and the model accuracy required. The aggregation and disaggregation approaches are included in the spatial scale (Blöschl & Sivapalan, 1995). The aggregation approach represents the heterogeneity of parameters (e.g. soil texture) as an averaged value for the entire basin, and performs averaged results and behavior of large-scale processes (Cohen et al., 2013). Alternatively, the disaggregation approach represents basin heterogeneity better, resulting in a more detailed model that can characterize knowledge gaps in sediment fluxes in large-scale regions (Vigiak et al., 2017). A recent study highlighted the significance of large-scale employments and their inherent relationship in processes between scales, which can aid in the understanding of uncertainties (Alewell et al., 2019). To reduce model complexity due to scale, we frequently use the Hydrological Response Units (HRU) approach, which groups calibration parameters by homogeneous zones based on the physical characteristics that influence water processes (Flügel, 1995; Kumar et al., 2013). The hydrological modeling studies are based on physical-ecological properties that mostly represent water

processes, as reflected by the calibrated parameters (Flügel, 1995; Poblete et al., 2020). Even in hydro-sedimentological modeling, the emphasis is on water processes, with the HRU approach used to calibrate the model (Fagundes et al., 2019).

Some applications of the combined conceptual hydrological model with the MUSLE, according to Sadeghi et al. (2014), have resulted in errors due to a lack of calibration (Sadeghi et al., 2014). According to Sadeghi et al. (2014), only 22% and 28% of the 48 analyzed studies between 1977 and 2012 calibrated the coefficient (α) and the power coefficient (β), respectively. Furthermore, 28% of the studies did not revise the coefficients and did not emphasize the importance of calibration. 39% of 41 studies revised between 2015 and 2020 (details in Supplementary Material) used distributed structure, with HRU (Djebou, 2018; Vigiak et al., 2015), sub-basins/catchments (Barik et al., 2017; Kumar et al., 2018), or both (Fagundes et al., 2019). Location coefficients have only been calibrated by Fagundes et al. (2019). However, the authors only calibrated sub-basins and did not include the HRU groups in the calibration procedure. Half of the studies with distributed structure used the HRU technique, which focused on hydrological modeling. Even when the model used an HRU structure with sediment-parametrization factors like soil texture (Samad et al., 2016), it is affected by the catchment scale. As a result, instead of developing hydrosedimentologically similar regions, these models generated a large number of HRU (Qi et al., 2017; Samad et al., 2016; Djebou, 2018), increasing the complexity and overparameterization. As a result, when using the model to forecast changes in environmental conditions, it may generate conflicting results (Beven & Binley, 1992; Kirchner, 2006).

The typical difficulty of obtaining satisfactory results from large-scale modeling (Furl et al., 2015; Qi et al., 2017; Fagundes et al., 2019) can be attributed to the lack of observed data and strategies to perform calibration in hydro-sedimentological modeling, the scale variability, and the difficulty in representing the heterogeneity of sediment-process characteristics. For improved outcomes, calibration strategies for hydro-sedimentological model applications must be developed and planned (Sadeghi et al., 2014; Franco et al., 2020). Fagundes et al. (2019) discussed how changing the spatial scale might enhance results. By integrating meteorological information into HRU, Poblete et al. (2020) have demonstrated increases in hydrological modeling scores and computing efficiency. Therefore, the current study attempts to investigate calibration strategies with an emphasis on discretization features, such as spatial scale and HRU approaches.

Given the scarcity of hydro-sedimentological large-scale models calibration testing in the currently available literature, we focused on five major themes in this research: (1) the creation of a large-scale HRUSed input map for hydro-sedimentological modeling; (2) the question whether employing a basic sediment-focused HRU technique (called HRUSed) to prepare the model can maintain hydrological modeling quality to a satisfactory level as with a purely HRU approach; (3) whether a calibration strategy based on the sediment discretization approach (HRUSed) can more accurately represent the results for suspended sediment concentration (SSC) and suspended sediment discharge (SSD); (4) the use of SSC versus SSD data for model calibration; and

(5) the trade-offs between increasing the spatial resolution of the large-scale model and employing the suggested HRUSed.

To accomplish this, we created a Hydro-sedimentological Response Units map (HRUSed) for South America and used it in conjunction with several basin sizes to calibrate the MGB-SED model, a hydro-sedimentological model from the standpoint of large-scale regional modeling. The main results of this study are: (1) the database of continental HRUSed map; (2) an analysis of whether using HRUSed or HRU maintains quality and performs similarly in hydrological modeling; (3) if the HRUSed map produces superior results for modeling sediment transport; (4) comparisons of the outcomes of SSC and SSD calibration; and (5) comparing the outcomes of the HRU and HRUSed techniques with basin-discretization improvements.

MATERIAL AND METHODS

Figure 1 shows a flowchart of the methodology applied in this study. Each methodological stage is then discussed in more detail.

Hydro-sedimentological Response Units map for South America (HRUSed)

With an emphasis on soil texture and land cover, we created a Hydro-sedimentological Response Units map (HRUSed) for South America. We selected the texture attribute since it is a stable and easily available data source (An et al., 2016). Since some variables, including hydraulic conductivity and porosity, depend on grain size, it is coherent with hydrological modeling (Maidment, 1993; U.S. Department of Agriculture, 2009). Additionally, it is important information for conceptual models that use empirical equations like USLE (Wischmeier & Smith, 1978), MUSLE (Williams, 1975) and RUSLE (Renard et al., 1997) that use soil texture to calculate the erodibility factor (K) (Arnold et al., 1998; Buarque, 2015).

For all South America, we used the FAO Soil Texture Map (Batjes, 2005), which was created in 1998 and has a spatial scale is of 1:50 km. However, when more precise maps were available, they were used, as in the case of Brazil and Argentina. We utilized the 1:2.5 km-scale soil texture map from IBGE, the *Instituto Brasileiro de Geografia e Estatística* (Instituto Brasileiro de Geografia e Estatística, 2018), for Brazil. In much of Argentina, we used the 1:5 km-scale Argentine Soil Texture Map from GeoINTA – *Instituto Nacional de Tecnología Agropecuaria* (Instituto Nacional de Tecnología Agropecuaria, 2013). Using *GIS software*, we combined all the maps and stacked the highest quality map on top. “Water Bodies”, “Sandy Soil” (clay percentage ranges from 0 to 15%), “Medium Soil” (clay percentage varies from 15 to 35%), “Clay Soil” (clay percentage is more than 35%), “Semi-Waterproof Soil”, and “Flooded Areas” are the groups we assigned based on the texture and water importance.

We used the land use and cover map from ESA GlobCover Portal (European Space Agency, 2018) for the year 2009. Envisat’s MERIS sensor, which has a 300 m grid resolution composition, revealed 22 classifications. We reclassified the map into: “Flooded Areas/Meadow” for post-flooding or irrigated croplands, flooded

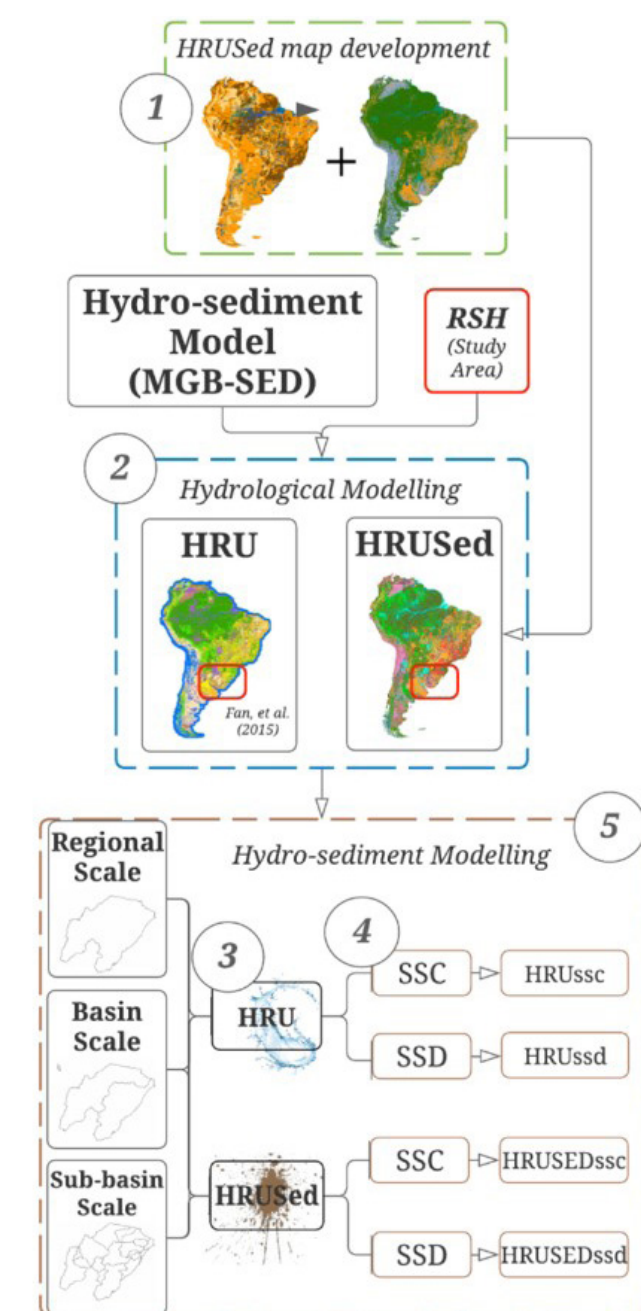


Figure 1. Flowchart of the methodology showing the process. The numbers correspond to the goals of the study, which were as follows: (1) the creation of a large-scale HRUSed input map for hydro-sedimentological modeling; (2) the hydrological modeling experiment between HRU (Fan et al., 2015) and HRUSed; (3) the experiment for each scale using SSC versus SSD as variable to calibrate the model; (4) the experiment for each scale using HRU versus HRUSed as discretization approach to calibrate the model; and (5) the trade-offs between discretization model approaches. The study area is the red rectangle.

forests, shrubland, grassland and woody vegetation; “Croplands” for rain-fed croplands, mosaic, and vegetation; “Grasslands” for a mosaic of vegetation and cropland, grasslands and forest/shrubland, herbaceous vegetation, sparse vegetation and bare areas; “Forest” for semi-deciduous, deciduous and evergreen forests,

mixed broadleaved and needle-leaved forest, mosaic of forest/shrubland, grassland and shrubland; “Semi-Waterproof Areas” for artificial surfaces, urban areas and permanent snow and ice areas; and “Water Bodies” for water resources. The soil texture and land use maps may be found in the Supplementary Material.

Utilizing *GIS software*, we merged the soil texture map and the land use map. We first produced a large number of HRUSeds. To avoid overparameterization, we reduced this number to 12 Hydrosedimentological Response Units (HRUSed) categories for South America. Fewer classes make calibration easier since they lower the number of calibration parameters and give the discretization a spatial component (Anand et al., 2018). The HRUSed map for Rio Grande do Sul hydrological (RSH), created for South America, is shown in Figure 2. You may download the map in <https://doi.org/10.5281/zenodo.7338417>.

Hydrosedimentological modelling

Study area

The southernmost Brazilian territory in South America is the Rio Grande do Sul state (RS) (Figure 3). The Patos Lagoon

basin (PL) (Lopes et al., 2018) and the Uruguai River basin (UR) (Fan et al., 2017) are the two major watersheds, with a combined drainage area of over 480,000 km². With 11 million residents, the RS state ranks fourth among Brazilian states in terms of economic output. Additionally, RS has grown the planted area of its soybeans by more than 50% between 2008 and 2018 (Rio Grande do Sul, 2019). These activities may result in the loading of contaminants or the loss of the fertile layer. Some rivers are used as sources for mining sediments, which can have an adverse effect on the ecosystem. In addition, during severe rains, increased sediment movement at water treatment plant input locations, can raise expenses and complicate the water treatment procedure.

The climate is Temperate, Subtropical and Humid Mesothermal according to Köppen’s classification (Rio Grande do Sul, 2019). The yearly average temperature is from 15°C to 18°C (Rio Grande do Sul, 2019), while the annual average rainfall ranges from 1,250 mm/year to 2,000 mm/year (Instituto Brasileiro de Geografia e Estatística, 1977). Atlantic Forest and *Pampa* biomes are found in the Rio Grande do Sul Hydrological region (RSH). The northernmost portion of the territory is covered by Atlantic Forest, while the remaining parts are found in conservation areas (Lopes et al., 2018; Rio Grande do Sul, 2019). *Pampa* covers the southern part of RSH and is characterized by grassland vegetation.

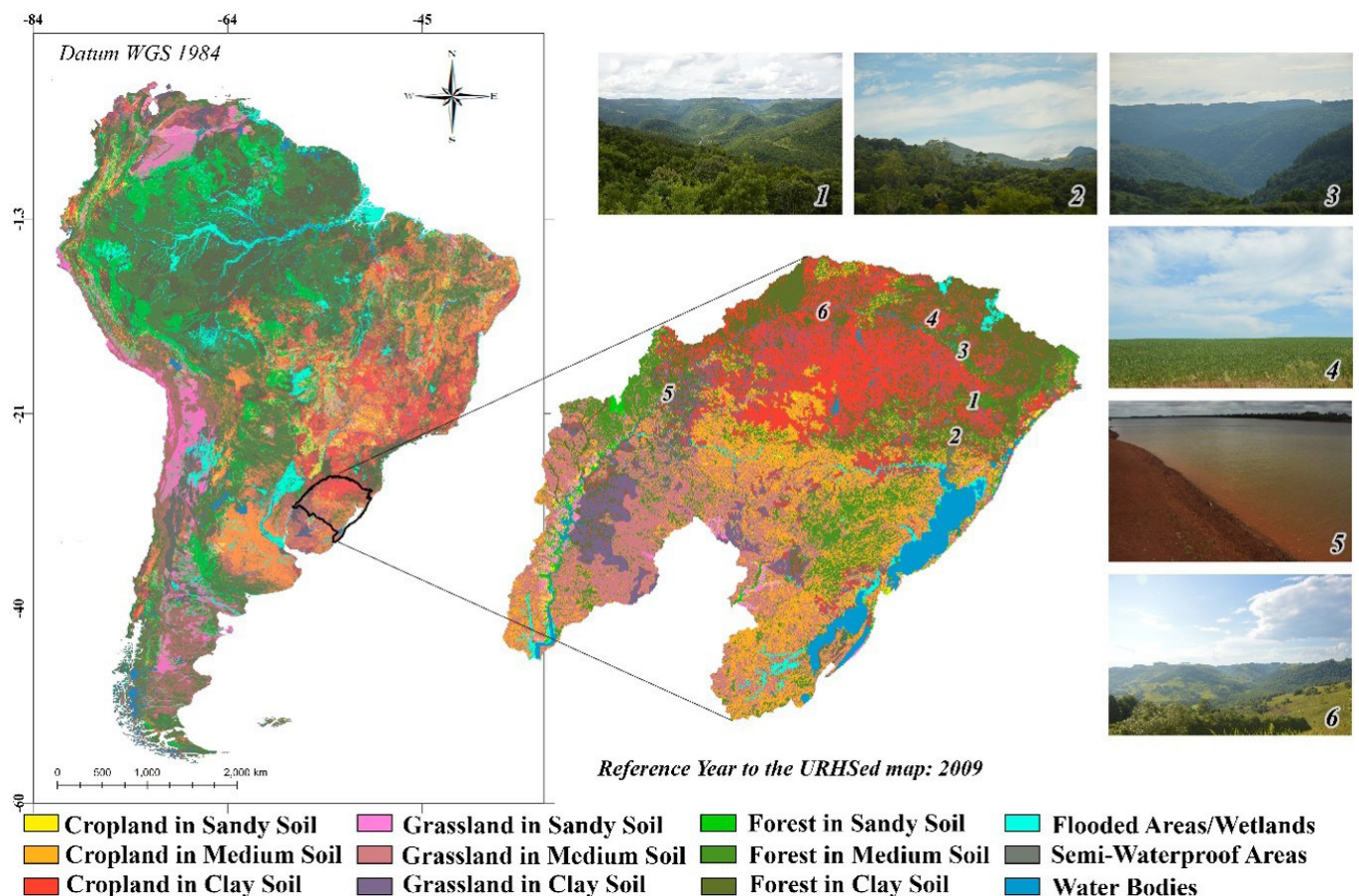


Figure 2. HRUSed map for South America and the Rio Grande do Sul hydrological (area for modeling study with more details in the study area section). The reference map is for the year 2009. The photos were taken in the Patos Lagoon basin and Uruguai River basin in January 2019 and 2020. (1) Caí River valley; (2) Relief in Sinos River basin; (3) Relief in Pelotas River basin; (4) Land uses in Canoas River basin; (5) Clay soil and flooded areas in Uruguai River basin; (6) Relief and land use in Uruguai River basin.

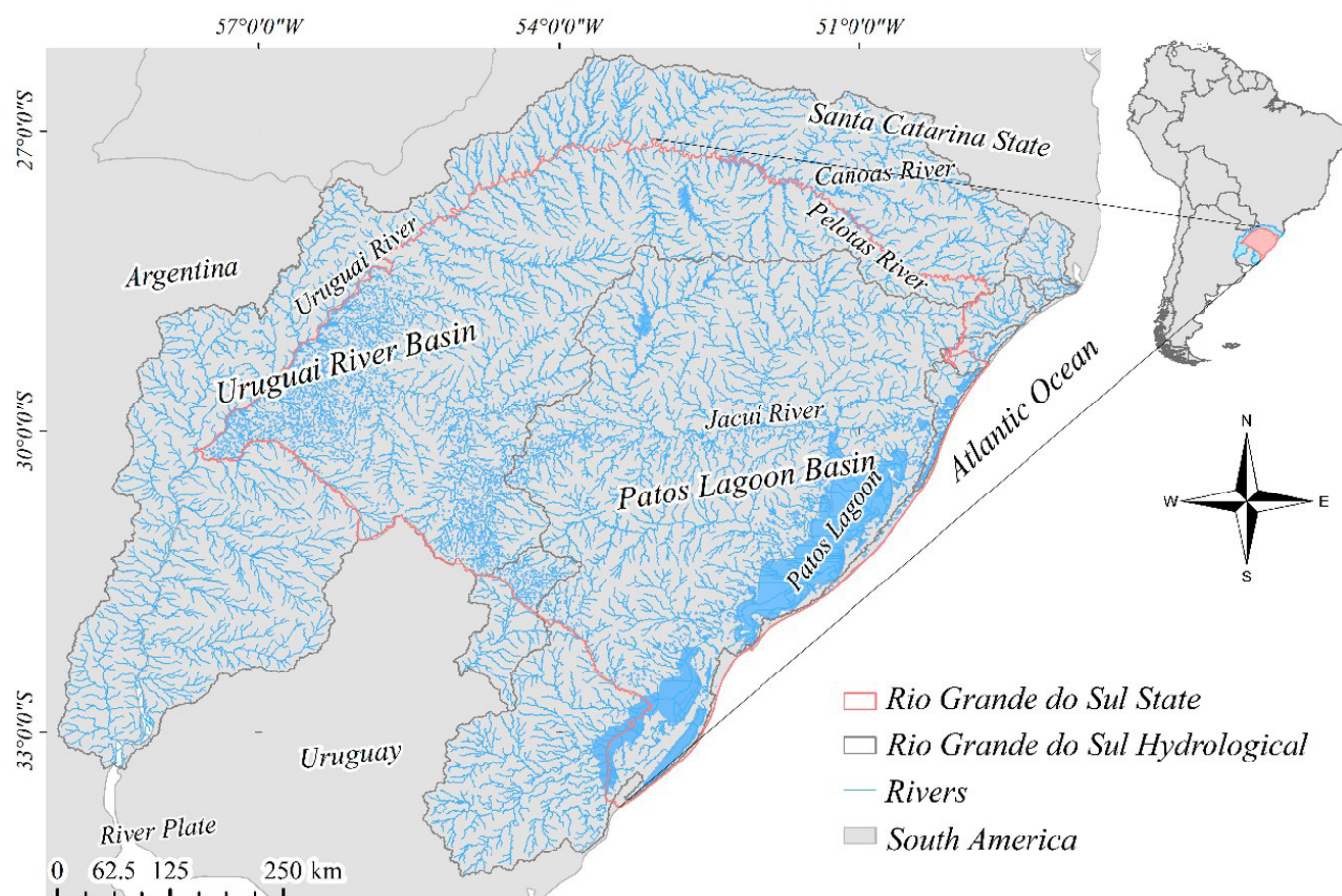


Figure 3. Localization of Rio Grande do Sul state (RS), southernmost Brazil. The red line is the limit of RS, and the grey line is the limit of the hydrological region of RS (RSH). Blue lines represent the rivers.

The relief of the headlands is hilly, with hydropower plants (Fan et al., 2017), and floodplains below.

The drainage areas of the Patos Lagoon basin and the Uruguai River basin are 180,000 and 275,000 km², respectively. The streamflow of the Jacuí River ranges from 380 m³/s to 1,300 m³/s (Vaz et al., 2006). The Uruguai River is formed by the confluence of the Pelotas and Canoas rivers and extends for 2,200 km till it reaches the River Plate (Ministério do Meio Ambiente, 2006). The streamflow of the Uruguai River is 690 m³/s upstream and 4,865 m³/s downstream (Ministério do Meio Ambiente, 2006). The sediment dynamic of the Patos Lagoon basin are very varied, driven by soil texture (Antiqueira & Calliari, 2005). Some sediment dynamics investigations, such as estimation of suspended sediment transport in rivers (Hartmann et al., 2010; Sari et al., 2017), variability of sediment transport (Andrade Neto et al., 2012; Toldo Junior et al., 2006), erosive coastal processes (Barboza et al., 2009), the effect of rain events on mass movements (Rio Grande do Sul, 2017), and mathematical modeling estimation of suspended sediment (Rossoni et al., 2018), have been produced.

MGB-SED model

The MGB-SED is a sediment module (Buarque, 2015; Föeger et al., 2019) that has been included into the MGB hydrological

model (Collischonn et al., 2007; Pontes et al., 2017). It is a large-scale semi-distributed model that simulates hydrological processes at the daily level using physical and conceptual equations (Paiva et al., 2011). The MGB has been subdivided into basins, sub-basins, and small unit-catchments (Fan & Collischonn, 2014). It also employs the concept of hydrologically homogeneous regions, abbreviated HRU (Hydrological Response Units). They are often a mix of land use/cover and soil types based on soil storage capacity (Fan et al., 2015; Pontes et al., 2017). In this study, we substituted HRU with HRUSed, which are hydro-sediment-focused homogeneous areas. The model calculates water and energy for each HRUSeds in each catchment, each with its own river length, simulating river routing mechanisms (Pontes et al., 2017). The inertial approach proposed by Bates et al. (2010) is used for flow propagation in the river network. Further details are available on Collischonn et al. (2007), Fan & Collischonn (2014) and Pontes et al. (2017).

The MGB-SED consists of three significant modules: basin, river, and floodplain. Using the MUSLE (Williams, 1975), the basin module simulates soil detachment and transport from catchment to river. The river module employs the advection equation to calculate the transport of suspended sediment (silt and clay particles) without deposition or erosion (Fagundes et al., 2020b). The Exner equation is used to describe bedload transfer (sand particles) and deposition or erosion of sediments in the river bed (Buarque, 2015). Using the Yang equation, channel

erosion and deposition are estimated as a function of the sediment transport capacity of the stream flow (Fagundes et al., 2020b). The floodplain module is a simple storage area for the interchange of fine sediments with the main river (Buarque, 2015). Equation 1 shows the MUSLE for each HRUSed pixel in each small unit-catchment to estimate sediment yield.

$$SED_{i,j} = \alpha \left(Q_{suri,j} \cdot q_{peak,i,j} \cdot A_{i,j} \right)^\beta \cdot K_j \cdot C_j \cdot P_j \cdot LS_{i,j} \quad (1)$$

Where, SED [$t \text{ d}^{-1}$] is sediment yield, Q_{sur} [$\text{mm} \text{ d}^{-1}$] is surface flow volume, q_{peak} [$\text{m}^3 \text{ s}^{-1}$] is peak surface flow rate, A [ha] is pixel area, K [$0.013 \text{ t m}^2 \text{ h} / (\text{m}^3 \text{ t cm})$] is soil-erodibility factor, C [-] is the cover management factor, P [-] is erosion-control-practice factor, LS [-] is slope length and gradient factor, α [-] and β [-] are location coefficients, i [-] and j [-] are indexes that indicate small unit-catchment and HRUSed, respectively.

The MGB-SED calculates the LS factor for each pixel, based on DEM (Digital Elevation Model) (Buarque, 2015), using the Desmet & Govers (1996) approach for the slope length factor (L) and the Wischmeier & Smith (1978) method for the slope steepness factor (S). The soil-erodibility factor (K) was calculated using the Sharpley & Williams (1990) equation. Based on the texture of each HRUSed, we approximated the percentages of clay, sand and silt. Cropping management factor (C) is connected to land cover and use. Based on the literature, we assigned 0.10 to cropland (Branco, 1998; Silva et al., 2011), 0.02 to grasslands (Branco, 1998), 0.0001 to forests, flooded areas and wetlands (Branco, 1998; Carvalho, 2008), and 0.1 to semi-waterproof regions, considering urban areas and bare soil (Farinasso et al., 2006). The erosion-control-practice factor (P) represents soil management effects. Due to a lack of information, we assumed it was equal to 1 (Bagherzadeh, 2014).

We calibrated the parameters α and β (Equation 1) and \forall (Equation 2). Coefficients α and β are location-specific conceptual factors from MUSLE that can only be obtained by adjusting the model (An et al., 2016). In the MGB-SED model, the sediment yield is routed to stream network using simple linear reservoir for each soil granulometry class (Fagundes et al., 2020b). We estimated the travel time of linear reservoirs for each soil granulometry class of sediments discharge to the drainage network using the correction factor (\forall) (Equation 2) (Fagundes et al., 2020b).

$$t = V \cdot TKS \quad (2)$$

Where, TKS [s] represents the delay time of surface linear reservoir output; t [s] represents travel time of sediments to drainage network; and V [-] is the adjustment factor for the two parameters. The ranges of the calibrated parameters were 0.01-25.0 (α), 0.1-0.5 (β), and 0.1-5.0 (V).

We utilized the MOCOM-UA (Yapo et al., 1998) optimization technique. We used 100 individuals to test each population, with a maximum iteration of 1000. For the optimization procedure, we specified three objective functions (Section “Calibration experiments”). Fagundes et al. (2019) performed automated calibration in MGB-SED based on catchment-scale variability. We attempted a more physically coherent calibration by supplementing the automatic calibration by concentrating on scale variability, not only on catchment scale but also on Hydro-sediment Response Units (HRUSed).

Data set

We obtained spatial information such as flow direction, accumulated drainage area, and streamflow network using SRTM DEM (*Shuttle Radar Topography Mission*) (Farr et al., 2007) with 90 m of grid spacing (Figure 4a). The model was subdivided into nine basins (Figure 4c), 30 sub-basins (based on main tributaries), and 8649 unit-catchments (Figure 4d), which were the smallest portion of the model discretization. Furthermore, we discretized into HRU (Hydrological Response Unit map) (Fan et al., 2015) and HRUSed (Section “Hydro-sedimentological Response Units map for South America (HRUSed)”) maps to compare hydrological and hydro-sedimentological discretization methodologies. We used climatic data from 44 INMET (*Instituto Nacional de Meteorologia*) meteorological stations acquired from the MGB model dataset (Fan & Collischonn, 2014). Air temperature, relative humidity, atmospheric pressure, wind speed, and insolation are all included.

We also used data from 549 rain gauge stations, 117 fluvimetric stations, and 60 sedimentometric gauge stations (Figure 4b) from the “Hidroweb” Brazilian database from ANA (*Agência Nacional de Águas*), which we accessed between 2017 and 2018. For each unit-catchment, we interpolated daily rain data, using the inverse of distance weighted (IDW) method, and computed suspended solid discharge ($SSD - \text{t/d}$) from suspended sediment concentration ($SSC - \text{mg/l}$) and streamflow ($Q - \text{m}^3/\text{s}$) (Equation 3). SSC , SSD , and streamflow from observed data were compared to simulated data.

$$SSD = 0.0864 \times Q \times SSC \quad (3)$$

Model evaluation

Using Nash-Sutcliffe Efficiency (NSE) (Equation 4) and Volumetric Error Percentage ($PBLAS$) (Equation 5), we analyzed the hydrological model (Table 1). NSE is suitable for continuous long-term simulations and may assess how effectively the model replicates variations. However, NSE cannot assist in identifying model bias simply (Moriassi et al., 2015). Therefore, $PBLAS$ was used to assess the accuracy of the model’s estimations of average magnitudes (Moriassi et al., 2015). Kling-Gupta Efficiency (KGE) (Gupta et al., 2009) was used to analyze hydro-sedimentological findings owing to the limited number of in situ sediment data, since NSE is often used to historical series with larger data (Fagundes et al., 2019). We interpreted KGE values higher than -0.41 as an indication that the model outperformed the yearly average data used as a benchmark (Knoben et al., 2019). Observed and predicted values are denoted by O and P , respectively.

Calibration experiments

Hydrological calibration

We carried out a regional-scale automated calibration experiment using (1) Hydrological Response Units (HRU) (Fan et al., 2015) and (2) Hydrosedimentological Response Units (HRUSed). To produce a less biased outcome, we used automated calibration.

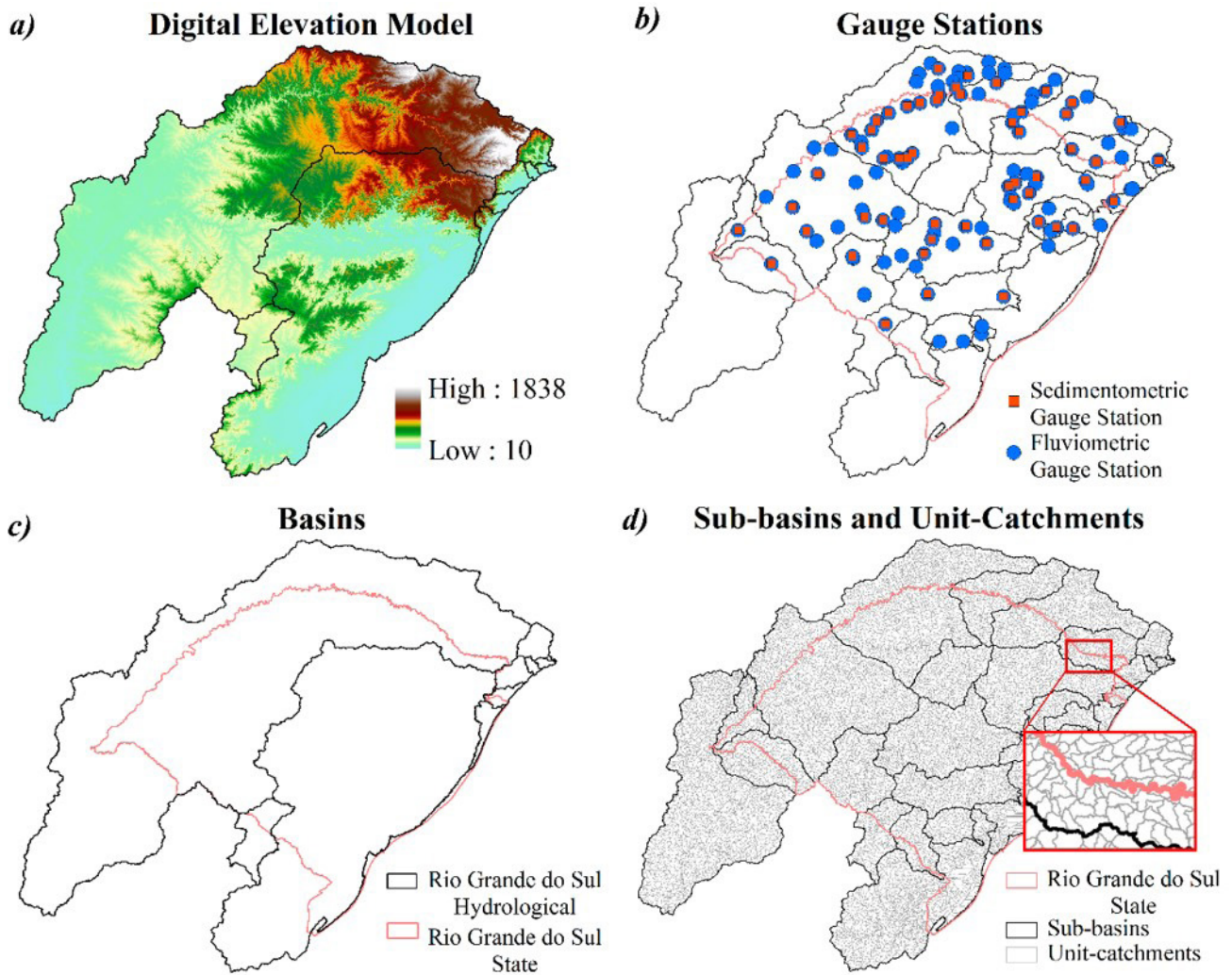


Figure 4. Data set for hydrological and hydrosedimentological models.

Table 1. Metrics used for statistical evaluation of the model. The benchmark column contains the value when the model is considered superior to the observed data mean. *NSE* is the Nash-Sutcliffe Efficiency, *PBLAS* is the percentage of volumetric inaccuracy, and *KGE* is the Kling-Gupta Efficiency.

Statistical Metric	Unit	Equation	Optimal Value	Benchmark	
<i>NSE</i>	-	$1 - \frac{\sum_{i=1}^n (O_i - P_i)^2}{\sum_{i=1}^n (O_i - \bar{O})^2}$	1	0	(4)
<i>PBLAS</i>	%	$\frac{\sum_{i=1}^n (O_i - P_i)}{\sum_{i=1}^n O_i} \cdot 100$	0	-	(5)
<i>KGE</i>	-	$1 - \sqrt{(r-1)^2 + (a-1)^2 + (b-1)^2}$	1	-0.41	(6)

Both models were calibrated using the same initial parameters values. The calibration and validation periods were respectively from 2000 to 2010 and from 1990 to 1999. We employed 117 and 106 gauge stations providing data for calibration and validation,

respectively, to analyze the results. We employed two objective functions: *NSE* (Nash-Sutcliffe Efficiency) and *BIAS* % (*BIAS*). We first calibrated the model using the Muskingum-Cunge approach (Collischonn et al., 2007) since it is a more simplified method

for flow routing, and afterwards we used the Inertial method (Pontes et al., 2017) to get better results in flooded regions.

Hydro-sedimentological calibration

We performed automated calibration tests for three distinct geographical scales: (1) regional scale, (2) basin scale, and (3) sub-basin scale (Figure 5). The purpose was to compare the influence of spatial scale discretization. We conducted four experiments for each spatial scale, each with a different process-focused discretization strategy (HRU versus HRUSed) and calibration variable (SSC versus SSD): (i) HRU_{SSC}, (ii) HRU_{SSD}, (iii) HRUSED_{SSC}, and (iv) HRUSED_{SSD} (Figure 1).

We calibrated the models using the same initial parameters values. We conducted experiments at several gauge stations since five sites lacked data for the calibration period. To eliminate gauge stations from calibration, we employed two or more of the following criteria:

- (a) Sub-basins with two or fewer gauge stations: (1) Calibration stations having fewer than one observed data, regardless of drainage area; (2) stations having outlier points (KGE values less than -1 without calibration to SSC and SSD);
- (b) Sub-basins with more than two gauge stations: (1) stations with fewer than 15 observed data points; (2) stations with drainage areas smaller than 1000 km²; and (3) stations having outlier points (KGE values less than -1 without calibration to SSC and SSD).

Due to the risk of a skewed outcome due to extreme KGE values, we only used these criteria for regional and basin-scale assessments. Using data from 50 gauge stations, we calibrated regional and basin-scale experiments. We used all available data for the sub-basin scale experiment to enhance the amount of data for calibration. We removed stations that met one or more of the criteria listed in item (b) from the only sub-basins with more than 10 gauge stations. Using data from 54 gauge stations, we calibrated the sub-basin scale experiments. Finally, for all experiments, we used KGE terms as objective functions for all.

RESULTS AND DISCUSSIONS

Hydrological modelling

The assessment of the two discretizations demonstrates that the quality of the hydrological models may be maintained utilizing a basic HRUSed technique presented in this study. Figure 6 shows a map of calibration process assessment metrics for each gauge station for HRU (Fan et al., 2015) and HRUSed maps. They exhibited comparable NSE and BIAS performance, as well as comparable areas of superior and inferior performance. Both maps had a mean NSE of 0.6 and PBIAS values of 13.4% (HRU) and 12.7% (HRUSed). Fan et al. (2017) tested a flood forecasting model for the Upper Uruguai River by combining the MGB model with the HRU map (Fan et al., 2015). The average NSE achieved was 0.69, while the BIAS ranged from -0.4 to -30.2%. Table 2 provides the BIAS values for each gauge station, enabling the identification of gauge stations with positive and negative BIAS values. Lopes et al. (2018) evaluated a more detailed model including wind effects for the Patos Lagoon area. The majority of gauges in the northern region of the PL basin exhibited NSE values greater than 0.6, indicating superior performance. The model NSE in the south ranges between 0.2 and 0.6. The findings were inferior to those of Lopes et al. (2018), perhaps because the model was discretized less precisely. We considered the model calibration as consistent and comparable to previous works.

Figure 7 illustrates hydrographs obtained by HRU and HRUSed over the calibration period, from 2006 to 2008, allowing for a more detailed examination of the similarities of the findings. They exhibited little distinctions and are comparable to the observed data. Nonetheless, both models had a tendency to overestimate (underestimate) the peaks in flooded regions (steeper regions) (Figure 7-1, 7-2, 7-3). In addition, 50.4% of gauge stations demonstrated superior performance for HRUSed, compared to 49.6% for HRU. It demonstrates the feasibility of simulating hydrological processes, even with a discretization strategy centered on sediment dynamics, owing to the low sensitivity of large-scale daily streamflow simulations to parameterization approaches (Kumar et al., 2013). The results of the model validation using hydrological data may be found in the Supplementary Material.



Figure 5. Basin discretization of study area in each experiment. Regional scale, basin scale and sub-basin scale, respectively.

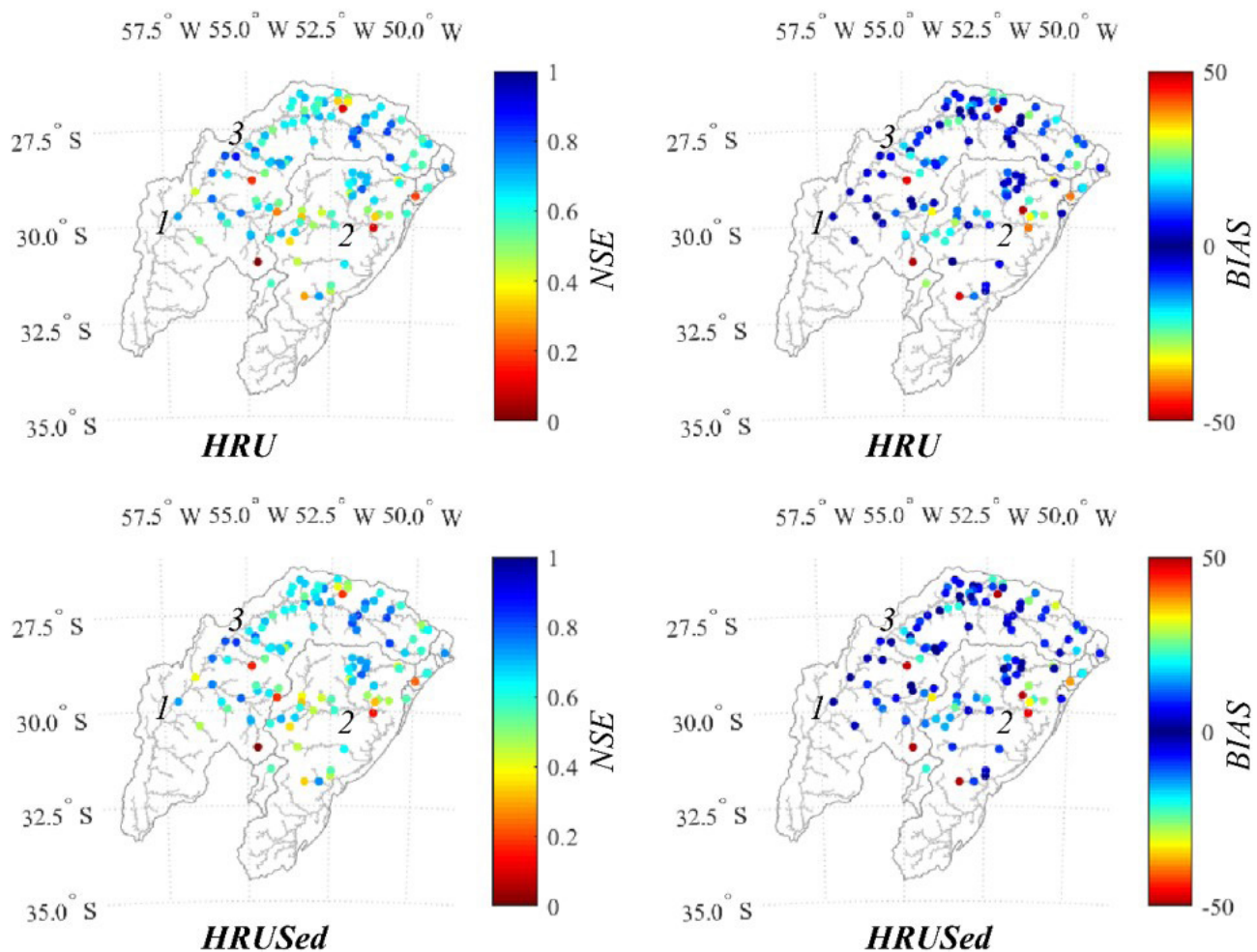


Figure 6. Hydrological model assessment for HRU and HRUSed maps calibration period. In spite of the fact that certain stations provided values < 0 for NSE, and > 50 and < -50 for BIAS, the scale was displayed up to these levels for improved readability. Stations with a brown hue indicated an NSE < 0 or BIAS > 50 or < -50 . The numerals 1, 2 and 3 relate to hydrographs illustrated in Figure 7. (1) Gauge station 77150000, located downstream in the Uruguai River; (2) Gauge station 85900000, located downstream in the Jacuá River, and (3) Gauge station 75500000, located in Ijuí River.

Hydro-sedimentological modelling

Calibration strategy based on discretization approach:
HRU x HRUSed

In every experiment, the HRUSed method yielded superior results for hydro-sedimentological modeling compared to the hydrologically-focused HRU method. From Figures 8-10, we reported the KGE values for SSC parameter calibration period for all experiments shown in Figure 5 (regional, basin and sub-basin scales). Despite the fact that a geographical comparison of both methodologies revealed comparable performance for calibration, as demonstrated in large-scale modeling (Kumar et al., 2013), the HRUSed map tended to provide more gauging stations with accurate findings. Due to regional scale calibration, the HRUSed method exhibited an averaged representation (Peters-Lidard et al., 2017). We observed this because KGE values ranging from -0.2 and

0.5 (light red to light blue) are more prevalent (Figure 8b and 8d). The HRU approach yielded a punctuated outcome, with better KGE values (blue points) in certain locations and lower values (dark red points) in others (Figure 8a and 8c).

The superior performance of the HRUSed technique was particularly apparent for the experiment conducted at the basin and sub-basin scales. We corroborated the averaged aspect of KGE results for HRUSed as well as the regional scale experiment. This indicates that compared to the HRU map, the HRUSed map had more values in the range of -0.2 to 0.5. Especially for the sub-basin experiment, the HRU technique showed more high KGE values and redder/oranger locations (Figure 10). Additionally, we improved the median value for KGE across all tests by using the HRUSed method (more details in Supplementary Material). We observed the same behavior with the SSD parameter experiment, however the KGE values were more consistent than the SSC findings. The findings are included in the Supplementary Material.

Table 2. BIAS values for each gauge station for the calibration period. We presented the values for each experiment using the HRU map and the HRUSed map.

Gauge Station	HRU	HRUSed
70100000	-25.8	-17.5
70200000	-9.9	-2.6
70300000	-14.3	-6.8
70700000	3.1	8.9
71200000	-26.6	-24.6
71250000	-10.8	-8.4
71300000	-11.0	-8.5
71490000	-19.3	-30.3
71498000	-10.1	-8.6
71550000	-10.9	-8.6
72300000	4.2	4.9
72430000	2.4	7.4
72630000	-0.5	2.7
72680000	-8.6	-6.0
72715000	9.6	12.7
72810000	26.2	26.9
72849000	0.9	3.7
72870000	-0.2	2.6
73300000	72.7	80.2
73350000	-7.0	-6.5
73550000	6.0	9.9
73581000	-24.5	-23.8
73600000	-23.2	-23.0
73690001	-7.0	-2.6
73693000	-13.1	-9.7
73765000	-0.5	-1.4
73770000	-6.9	-5.5
73780000	2.6	-1.5
73820000	13.7	9.8
73900000	17.4	14.3
73960000	0.6	1.1
74100000	-2.1	1.0
74205000	-3.9	2.9
74270000	-24.1	-21.1
74295000	0.0	-0.9
74300000	-6.9	-6.8
74320000	7.3	5.6
74370000	-24.2	-20.2
74422000	-11.7	-11.7
74424500	4.9	6.6
74470000	-2.7	0.4
74610000	5.2	4.1
74700000	-9.8	-9.9
74750000	8.1	5.6
74880000	1.8	1.4
74900000	-17.5	-18.9
75155000	-13.6	-7.8
75186000	-14.1	-7.7
75200000	-6.7	0.7
75205000	-7.2	-0.5
75230000	-16.4	-11.8
75295000	-11.7	-8.2
75320000	-20.1	-17.9
75400000	-21.7	-22.1
75500000	6.1	1.6
75550000	4.9	6.9
75600000	-46.9	-48.3

Table 2. Continued...

Gauge Station	HRU	HRUSed
75700000	6.6	-2.7
75780000	-4.1	-2.8
75900000	-2.1	0.0
76085000	3.8	5.2
76100000	13.7	12.6
76251000	-80.2	-81.2
76300000	13.1	3.8
76310000	18.4	10.4
76395000	32.2	34.0
76440000	-1.5	-0.1
76460000	0.7	-0.1
76500000	11.3	6.2
76742000	-3.3	-12.9
76750000	-1.0	-8.8
76800000	-3.0	-8.2
77150000	2.5	1.3
77500000	1.2	-2.9
79400000	27.1	21.2
84580000	-5.1	-7.6
84949800	-12.2	-13.9
84950000	-18.5	-19.6
84970000	-39.6	-37.1
85400000	-13.0	-8.8
85438000	-11.9	-14.1
85470000	17.4	12.1
85480000	22.0	16.6
85600000	28.5	24.1
85610000	21.4	15.8
85623000	19.1	14.3
85642000	2.3	3.1
85735000	3.8	6.1
85740000	15.7	13.4
85830000	20.3	21.4
85900000	7.9	7.5
86100000	-33.1	-27.6
86160000	-4.7	-1.2
86410000	-2.1	1.7
86420000	3.4	6.8
86440000	-3.0	0.6
86470000	3.8	7.4
86480000	11.9	16.6
86500000	4.4	8.6
86510000	-7.8	-4.6
86560000	-3.3	0.7
86580000	-16.4	-12.8
86700000	11.5	10.1
86720000	-8.3	-5.2
87160000	22.7	27.6
87170000	52.3	56.1
87317030	2.6	6.6
87374000	-28.9	-27.7
87380000	-21.9	-21.8
87382000	-32.2	-32.1
87450100	-39.9	-46.1
87590000	-0.8	-8.7
87905000	-5.8	-9.7
88575000	-47.2	-49.6
88641000	13.0	9.7
88750000	2.0	1.0
88850000	6.7	3.9

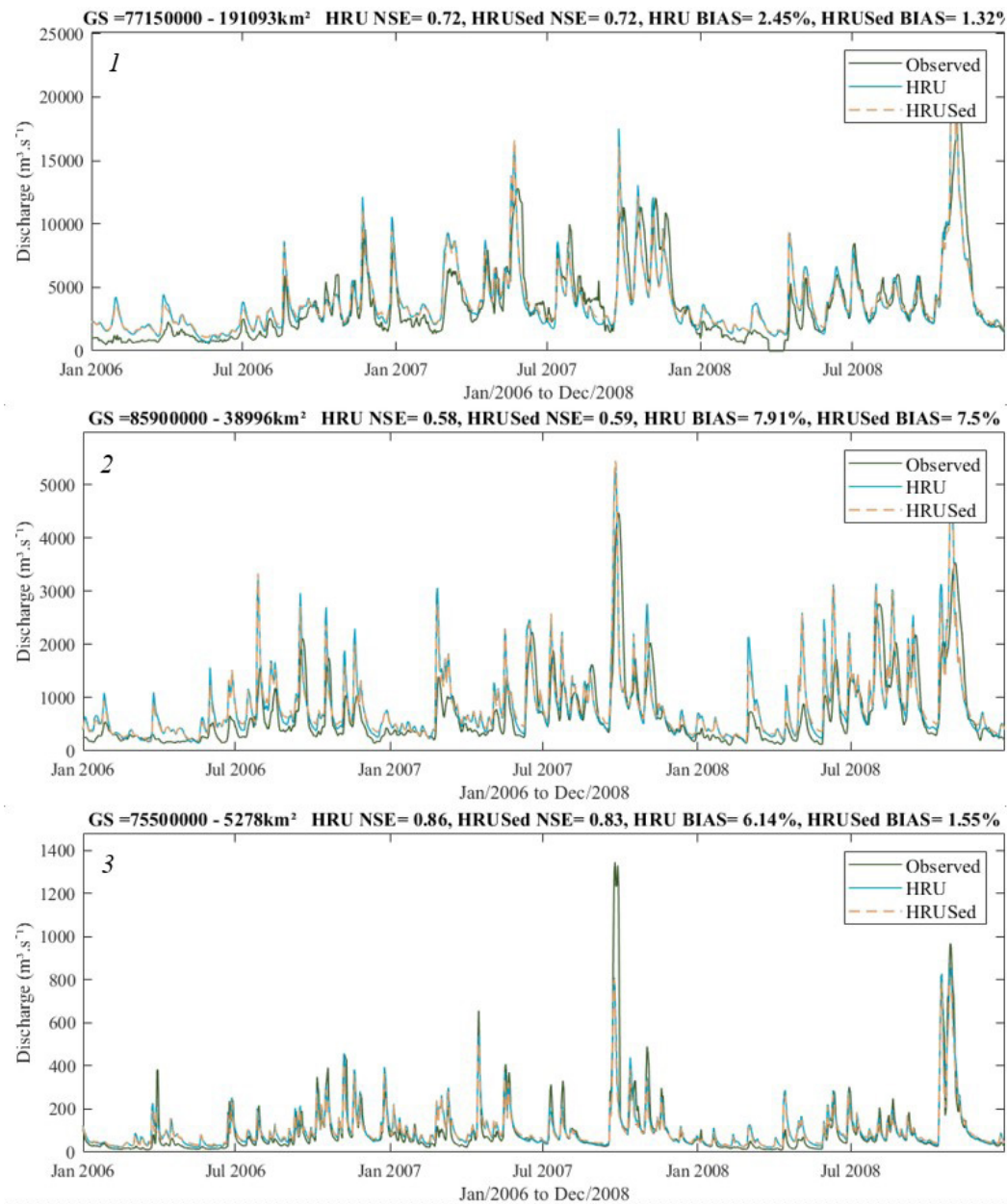


Figure 7. Hydrographs during the calibration period for observed data (green line), HRU model-simulated data (light blue line) and HRUSed model-simulated data (light brown dashed line). GS is the number of ANA gauge station and drainage area in km². The gauge station 77150000 is located downstream in the Uruguai River, the gauge station 85900000 is located downstream in the Jacuí River, and gauge station 77500000 is located downstream in the Ijuí River.

The utilization of SSC vs SSD data for model calibration period

Our findings indicate that calibrating the model using SSC and SSD enhanced both SSC and SSD when utilizing the HRUSed methodology. Using both SSC and SSD for calibration has mostly enhanced SSD for the HRU method, whilst SSC has seen just minor improvements. Figures 11-13 provide the cumulative distribution function for all spatial scales for the trials conducted (Figure 1). Low KGE values (< -1) were recorded for SSC and SSD findings. Nonetheless, they accounted for fewer than 8% (SSC) and 10% (SSD) of the total results (Figure 11). One gauge station showed

a KGE value less than -40 (SSD) in a small coastal catchment (350 km²), most likely because the model is not recommended for applications at small catchment sizes (< 1000 km²) owing to its inability to reflect the water subsuperficial flow across small catchments (Collischonn et al., 2007; Pontes et al., 2017). For models without calibration, the HRUSed method performed better than the HRU approach (Figures 11-13). It indicates that when performing the original MUSLE parameter adjustment, the hydro-sedimentological discretization method yields superior model performance.

For the regional scale experiment without calibration for the SSC parameter, more than 78% of stations had KGE values more than -0.41 (Knoben et al., 2019) for HRUSed, compared to

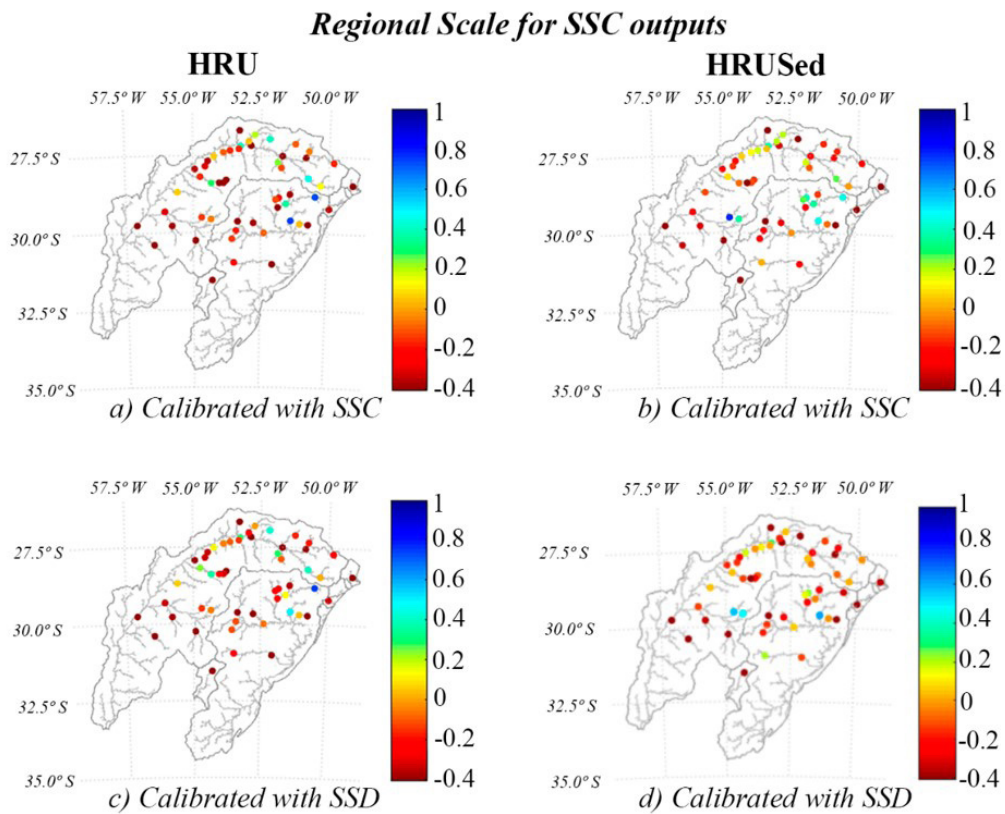


Figure 8. KGE values for SSC parameter throughout the regional test's period of calibration (2000 – 2010). Using (a) HRU and SSC, (b) HRUSed and SSC, (c) HRU and SSD, and (d) HRUSed and SSD for calibration. Limits between -0.41 to 1.

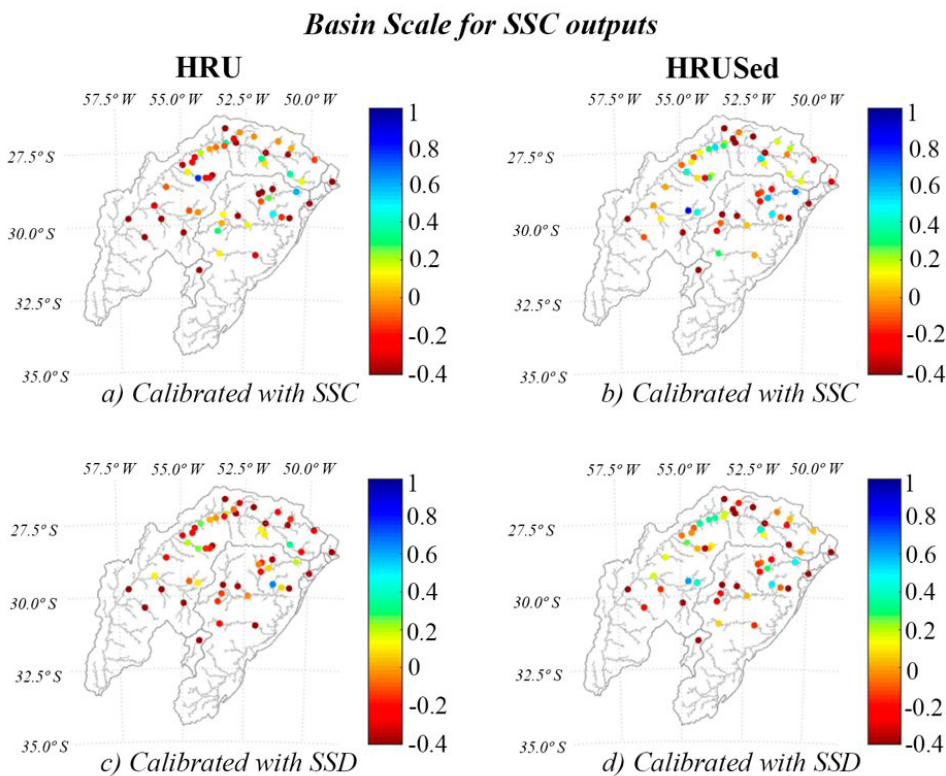


Figure 9. KGE values for SSC parameter for test at basin scale during calibration period (2000 – 2010). Using (a) HRU and SSC, (b) HRUSed and SSC, (c) HRU and SSD, and (d) HRUSed and SSD for calibration. Limits between -0.41 to 1.

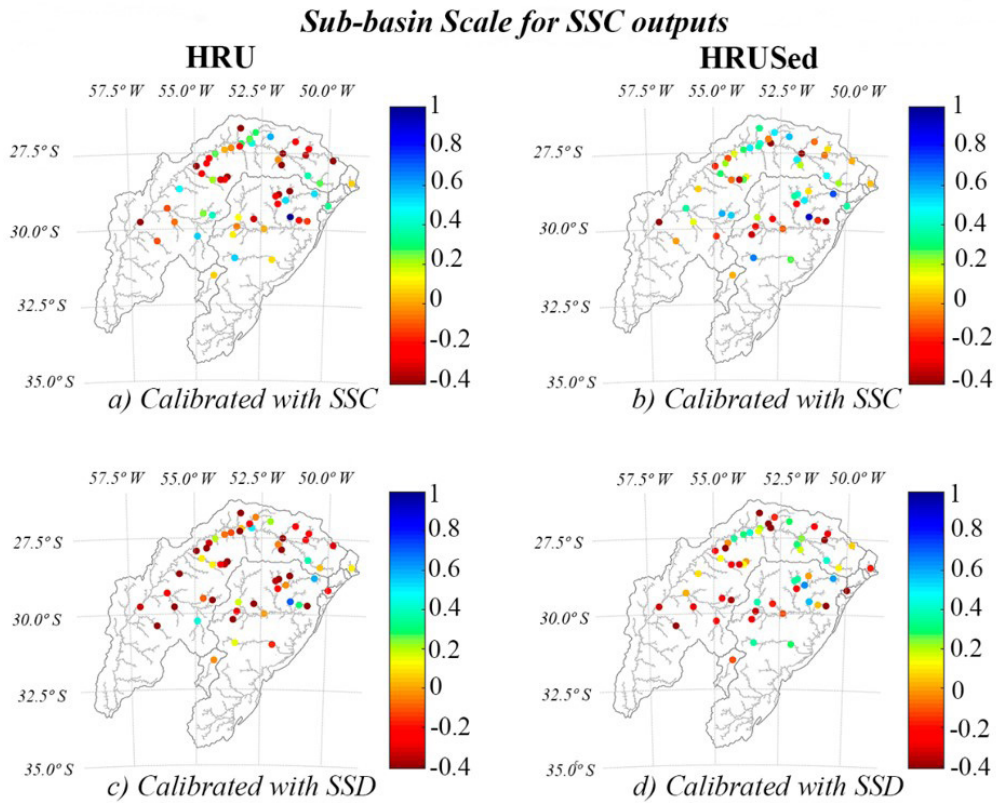


Figure 10. KGE values for SSC parameter for test at sub-basin scale during calibration period (2000 – 2010). Using (a) HRU and SSC, (b) HRUSed and SSC, (c) HRU and SSD, and (d) HRUSed and SSD for calibration. Limits between -0.41 to 1.

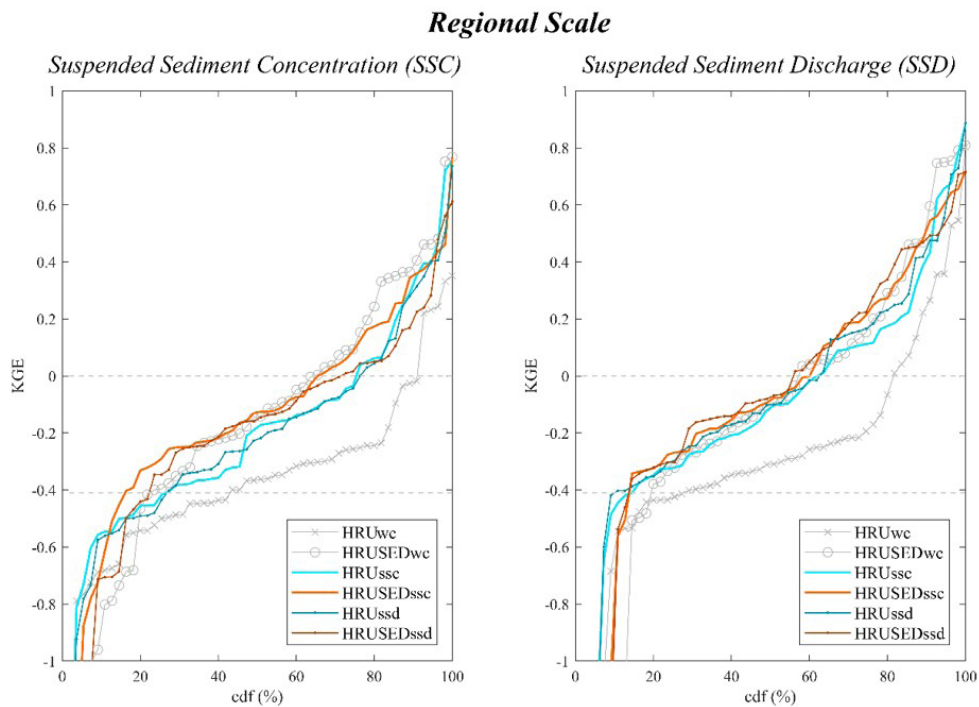


Figure 11. The cumulative distribution function (cdf) of KGE for SSC and SSD parameters is derived using the MGB-SED model for the calibration period, utilizing HRU and HRUSed and calibrating with SSC and SSD at a regional scale. Each line indicates an experiments: HRUwcc (HRU discretization without calibration), HRUSEDwcc (HRUSed discretization without calibration), HRUssc (HRU calibrating with SSC), HRUSEDssc (HRUSed calibrating with SSC), HRUssd (HRU calibrating with SSD) and HRUSEDssd (HRUSed calibrating with SSD).

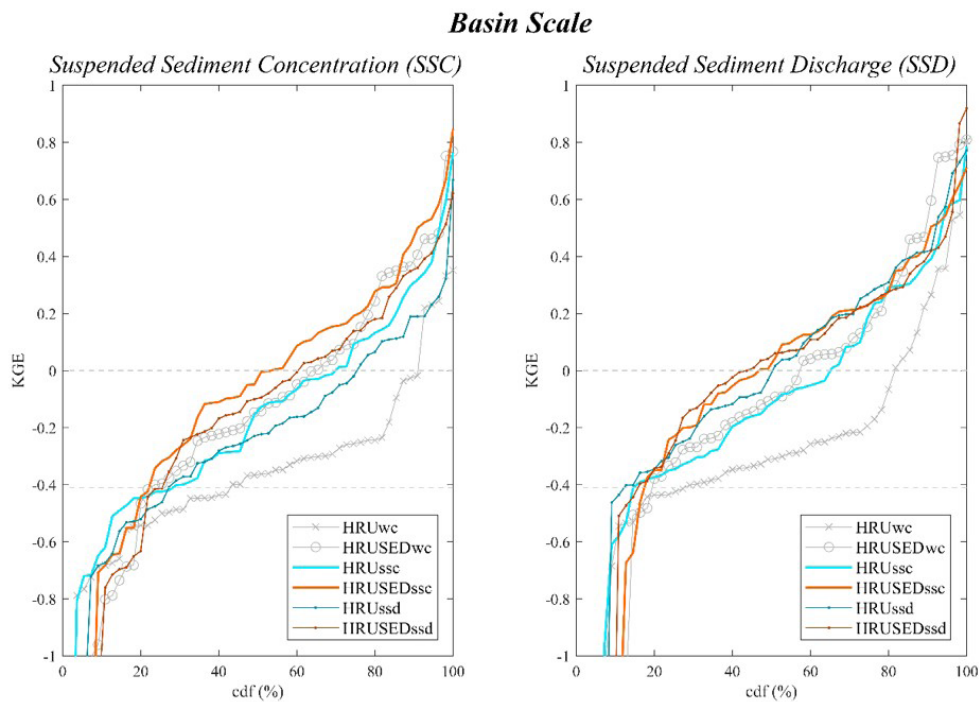


Figure 12. Cumulative distribution function (cdf) of KGE for SSC and SSD results from MGB-SED model for calibration period, using HRU and HRUSed, and calibrating with SSC and SSD for basin scale. Each line indicates an experiment: HRUwc (HRU discretization without calibration), HRUSEDwc (HRUSed discretization without calibration), HRUssc (HRU calibrating with SSC), HRUSEDssc (HRUSed calibrating with SSC), HRUssd (HRU calibrating with SSD) and HRUSEDssd (HRUSed calibrating with SSD).

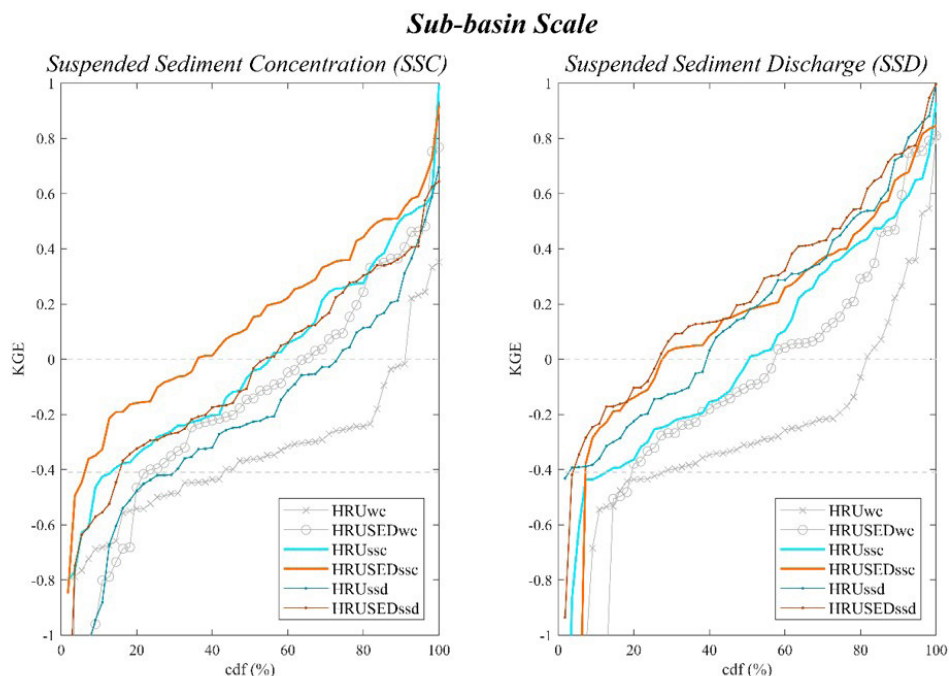


Figure 13. Cumulative distribution function (cdf) of KGE for SSC and SSD results from MGB-SED model for calibration period, using HRU and HRUSed, and calibrating with SSC and SSD for sub-basin scale. Each line represents the experiments: HRUwc (HRU discretization without calibration), HRUSEDwc (HRUSed discretization without calibration), HRUssc (HRU calibrating with SSC), HRUSEDssc (HRUSed calibrating with SSC), HRUssd (HRU calibrating with SSD) and HRUSEDssd (HRUSed calibrating with SSD).

57% for HRU. For the SSD parameter, we discovered values over 80.5% (HRUSed) and 72% (HRU). 84% (HRUSed + SSC), 78%

(HRUSed + SSD), and 74% (HRU + SSC/SSD) of the calibrated stations had KGE values higher than -0.41 for SSC parameter.

For SSD parameter, we observed values of 90% (HRU + SSD), 87% (HRUSed + SSC/SSD) and 86% (HRU + SSC). With the HRUSed method, we were able to generate more stations with higher KGE values for SSC than using the HRU method, but SSD values were comparable.

The cumulative distribution function (*cdf*) for KGE values in basin-scale studies was shown in Figure 12. In 78% of gauge stations with HRUSed and 72% of gauge stations with HRU, KGE values for SSC were more than -0.41 (Knoben et al., 2019) when calibrating with SSC. Using SSD for calibration, these values were 75% for HRUSed and 73% for HRU. In 88%, 85.5%, 84% and 82.5% of the gauging stations for SSD findings had KGE values greater than -0.41 for calibration with HRU+SSD, HRU+SSC, HRUSed+SSD, and HRUSed+SSC, respectively. We observed that the HRUSed discretization method (brown and orange lines) provided superior performance for SSC and SSD parameters in both plots.

The cumulative distribution function (*cdf*) for KGE for the sub-basin scale experiment is shown in Figure 13. HRUSed+SSC calibration produced the best outcome for SSC findings (orange line). HRUSed with SSD calibration and HRU with SSC calibration yielded comparable results. Calibrating using HRU with SSD produced the poorest result. The percentage of stations with KGE values larger than -0.41 (for SSC parameter results) were as follows: 94% (HRUSed + SSC), 87% (HRU + SSC), 85% (HRUSed + SSD), and 70% (HRU + SSD). The calibration with HRUSed+SSD yielded the best SSD parameter result (brown line with points), whereas the calibrations with HRUSed+SSC and

HRU+SSD yielded worse results, although they were comparable. 97.5% (HRU+SSD), 96.5% (HRUSed+SSD), 93% (HRUSed+SSC), and 87.5% (HRU+SSC) of the stations exhibited KGE values higher than -0.41 for the SSD parameter.

Integrated scale analysis: tradeoffs between enhancing the spatial resolution of the large-scale model and using the suggested HRUSed map

Figure 14 illustrates an integrated scale analysis for the calibration period. In general, the HRUSed method represented the heterogeneity of sediment dynamics more accurately. Through HRUSed's scales, we observed an improvement in SSC outcomes. An upscaling or large-scale representation of processes and parameters has an aggregated or averaged response while the outcome of a downscaling representation is distributed or detailed (Blöschl & Sivapalan, 1995; Peters-Lidard et al., 2017). This was noticed during the HRUSED_{ssc} experiment (Figure 14). With catchment downscaling (more detailed), we were able to increase the median values and reduce the interquartile range. It indicates that the model represents heterogeneity better when the scale is reduced (becomes more detailed) due to the loss of heterogeneity that occurs when merging small classes into bigger ones (Flügel, 1995).

We identified a “ladder effect” from the regional scale experiment (HRUSED_{ssc}-Reg) to sub-basin scale experiment

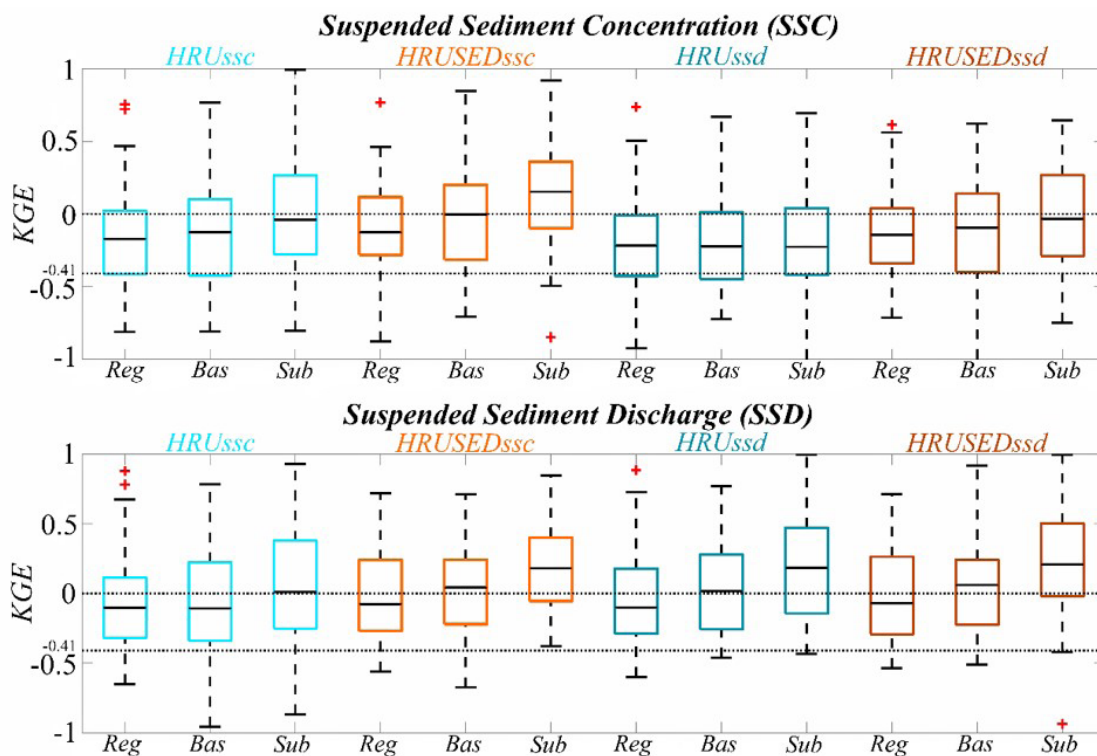


Figure 14. Integrated study of scales for calibration period. Box plots indicate KGE values for each experiment. Results for suspended sediment concentration (SSC) are on top, while suspended sediment discharge (SSD) is at the bottom. The lines with dots represent the values 0 and -0.41. Calibration with: HRU and SSC (light blue), HRUSed and SSC (orange), HRU and SSD (dark greenish-blue), HRUSed and SSD (brown). Experiments on scales: Reg (regional), Bas (basin) and Sub (sub-basin).

(HRUSED_{SSC-Sub}). For the other SSC experiments, we noticed that the median remained constant but the interquartile range varied considerably (HRU_{SSD} and HRUSED_{SSC}). The results of the HRU_{SSC} experiment were more comparable to those of the HRUSED_{SSC}. However, the median has not increased significantly, and the interquartile range has not demonstrated the “ladder effect” observed in the HRUSED_{SSC} experiment. For median and interquartile variations, both HRU_{SSD} and HRUSED_{SSD} exhibited the “ladder effect” for SSD findings. This implies that both methodologies improved with scaling when calibrating with SSD. With SSC calibration, the HRUSED_{SSC} performed better.

Consequently, the results show that only discretization at a lower scale has not resulted in more accurate representations of the processes. When the properties of the simulated processes are not well represented, we hypothesized that a reduction in scale would not result in an improvement. However, increased discretization tends to enhance outcomes when combined with a discretization process-focused strategy (Poblete et al., 2020), as seen in our work for the sediment-focused HRUSed. This is likely due to the fact that HRUSed does not yet adequately explain local processes, necessitating spatial discretization for better calibration. Utilizing HRUSed with a more detailed discretization approach is the preferred strategy.

To substantiate these results, we presented statistics for all experiments in Tables S3 through S5 of the Supplementary Material. We observed that the HRUSed method provided improved median KGE values across all tests (concerning spatial scale and the calibration variable). Despite the low median KGE values (ranging from -0.14 (HRUSED_{SSD} – regional scale) to 0.21 (HRUSED_{SSD} – sub-basin scale) and -0.22 (HRU_{SSC} – regional scale) to 0.18 (HRU_{SSD} – sub-basin scale)), it is a multi-site calibration strategy (Franco et al., 2020), and lower median values are expected when compared to a single KGE value resulting from a single-site calibration strategy (Fagundes et al., 2019; Kaffas & Hrisanthou, 2019).

Additional hydro-sedimentological model validation outcomes are available in the Supplementary Material (Figure S6). It is expected that the model with a larger physical base, such as HRUSed, would have a stronger potential for extrapolation. Nevertheless, validation results (Figure S6 of Supplementary Material) indicate that this was not the case. Although the sub-basin experiment’s HRUSED_{SSC} had fewer outlier values, the regional experiment’s SSC performance was superior (Figure S6 of Supplementary Material). Thus, incorporating the detailed spatial discretization calibration reduced the model’s extrapolation capability, as seen by the validation results. Due to the decreased extrapolation capacity in the validation findings, the tradeoffs between increasing the spatial resolution of the large-scale model and using the proposed HRUSed map must be examined in light of the model’s intended usage. According to the study’s findings, it is preferable to use a discretization that better represents the sediment process (such as HRUSed) depending on the application (e.g. how the model’s results will be extrapolated) and the level of detail required (e.g. if at larger or smaller scales) without significantly increasing the number of parameters (Qi et al., 2017; Samad et al., 2016; Djebou, 2018).

CONCLUSIONS

In erosion and sediment transport large-scale modeling, the lack of knowledge regarding calibration strategies is a limiting constraint. In order to help overcome this information gap, we investigated the use of discretization methodologies based on hydro-sedimentological (HRUSed – Hydro-sedimentological Response Units) and scale (regional, basin, and sub-basin) variability. The main results-based findings were:

- The comparison between HRU (hydrology-focused) and HRUSed (sediment-focused) techniques demonstrates that it is possible to retain the same level of hydrological modeling quality utilizing the HRUSed methodology described in this study.
- The HRUSed approach generated better calibration results for hydro-sedimentological modeling than using the hydrological-focused approach (HRU).
- In addition, our results show that calibrating the model with SSC and SSD parameters enhanced both SSC and SSD when utilizing the HRUSed approach. However, using the HRU method and utilizing both SSC or SSD parameters for calibration has mostly increased SSD while slightly enhancing SSC outputs.
- The findings indicate that a more detailed spatial discretization has not resulted in more accurate representations of the processes. When the properties of the simulated processes (sediment) are not well represented, reducing the scale size of the scale has little effect on the results (as in the HRU approach). However, increasing spatial discretization in conjunction with a process-discretization strategy centered on hydro-sedimentological dynamics (HRUSed) increased the performance of the model. Therefore, the ideal strategy for large-scale modeling is the employment of a HRUSed approach with more detailed spatial discretization.
- The HRUSed methodology may represent regional areas as averaged parameters and processes representation. In response to an increase in sub-basin divisions, the model produced more specific findings, indicating the best representation of hydro-sedimentological process heterogeneity.

Finally, we believe that this research will aid in planning calibration strategies and gaining a better knowledge of the issues associated with large-scale distributed modeling for hydrological and hydro-sedimentological applications. We demonstrated that a focus-sediment method enhanced erosion and transport modeling results and spatial representation without compromising hydrological performance. Future studies should investigate other techniques, including simultaneous calibration of hydro-sedimentological parameters and simultaneous calibration of multi-variables. Also, we will be able to test additional texture maps, such as the HWSDB database.

ACKNOWLEDGEMENTS

The authors want to thank CAPES (*Coordenação de Aperfeiçoamento de Pessoal de Nível Superior*) and CNPq (grant number:

305636/2019-7) for providing support for conducting this study. We also want to thank Joana Postal Pasqualini for her valuable comments and proofreading of this manuscript.

REFERENCES

- Ahbari, A., Stour, L., Agoumi, A., & Oualkacha, L. (2018). A simple and efficient approach to predict reservoir settling volume: case study of Bin El Ouidane reservoir (Morocco). *Arabian Journal of Geosciences*, 11(19), 591. <http://dx.doi.org/10.1007/s12517-018-3959-7>.
- Alewell, C., Borrelli, P., Meusburger, K., & Panagos, P. (2019). Using the USLE: chances, challenges and limitations of soil erosion modelling. *International Soil and Water Conservation Research*, 7(3), 203-225. <http://dx.doi.org/10.1016/j.iswcr.2019.05.004>.
- An, L. S., Liao, K. H., Zhou, B. H., Pan, W., & Chen, Q. (2016). Global sensitivity analysis of the parameters of the modified universal soil loss equation. *Applied Ecology and Environmental Research*, 14(4), 505-514. http://dx.doi.org/10.15666/aecer/1404_505514.
- Anand, J., Gosain, A. K., Khosa, R., & Srinivasan, R. (2018). Regional scale hydrologic modeling for prediction of water balance, analysis of trends in streamflow and variations in streamflow: the case study of the Ganga River basin. *Journal of Hydrology: Regional Studies*, 16, 32-53. <http://dx.doi.org/10.1016/j.ejrh.2018.02.007>.
- Andrade Neto, J. S., Rigon, L. T., Toldo Junior, E. E., & Schettini, C. A. F. (2012). Descarga sólida em suspensão do sistema fluvial do Guaíba, RS, e sua variabilidade temporal. *Pesquisas em Geociências*, 39(2), 161-171. <http://dx.doi.org/10.22456/1807-9806.35910>.
- Antiqueira, J. A. F., & Calliari, L. J. (2005). Características sedimentares da desembocadura da Laguna dos Patos. *Gravel*, 3, 39-46. Retrieved in 2022, December 12, from <https://repositorio.furg.br/bitstream/handle/1/2141/Caracter%20c3%adsticas%20Sedimentares%20da%20desembocadura%20da%20Laguna%20dos%20Patos.pdf?sequence=1&isAllowed=y>
- Arnold, J. G., Srinivasan, R., Mutiah, R. S., & Williams, J. R. (1998). Large area hydrologic modeling and assessment. Part I: model development. *Journal of the American Water Resources Association*, 34(1), 73-89.
- Bagherzadeh, A. (2014). Estimation of soil losses by USLE model using GIS at Mashhad plain, Northeast of Iran. *Arabian Journal of Geosciences*, 7(1), 211-220. <http://dx.doi.org/10.1007/s12517-012-0730-3>.
- Barboza, E. G., Tomazelli, L. J., Dillenburg, S. R., & Rosa, M. L. C. D. C. (2009). Planície costeira do Rio Grande Do Sul: erosão em longo período. *Revista de La Sociedad Uruguaya de Geología*, 15, 94-97.
- Barik, D. K., Singh, A. D., Sra, M. S., & Raja. (2017). Estimation of runoff and sediment yield from a small ungauged watershed using GIS and HEC-HMS. *International Journal of Civil Engineering and Technology*, 8(6), 517-527.
- Bates, P. D., Horritt, M. S., & Fewtrell, T. J. (2010). A simple inertial formulation of the shallow water equations for efficient two-dimensional flood inundation modelling. *Journal of Hydrology*, 387(1-2), 33-45. <http://dx.doi.org/10.1016/j.jhydrol.2010.03.027>.
- Batjes, N. H. (2005). *SOTER-based soil parameter estimates for Latin America and the Caribbean (version 1.0)*. Wageningen: ISRIC-World Soil Information.
- Benavidez, R., Jackson, B., Maxwell, D., & Norton, K. (2018). A review of the (Revised) Universal Soil Loss Equation ((R)USLE): with a view to increasing its global applicability and improving soil loss estimates. *Hydrology and Earth System Sciences*, 22, 6059-6086.
- Beven, K., & Binley, A. (1992). The future of distributed models: model calibration and uncertainty prediction. *Hydrological Processes*, 6(3), 279-298. <http://dx.doi.org/10.1002/hyp.3360060305>.
- Blainski, É., Porras, E. A. A., Garbossa, L. H. P., & Pinheiro, A. (2017). Simulation of land use scenarios in the Camboriú River Basin using the SWAT model. *Revista Brasileira de Recursos Hídricos*, 22, e33. <http://dx.doi.org/10.1590/2318-0331.011716110>.
- Blöschl, G., & Sivapalan, M. (1995). Scale issues in hydrological modelling: a review. *Hydrological Processes*, 9(3-4), 251-290. <http://dx.doi.org/10.1002/hyp.3360090305>.
- Branco, N. (1998). *Avaliação da produção de sedimentos de eventos chuvosos em uma pequena bacia hidrográfica rural de encosta* (Master's thesis). Universidade Federal de Santa Maria, Santa Maria.
- Buarque, D. C. (2015). *Simulação da geração e do transporte de sedimentos em grandes bacias: estudo de caso do rio Madeira* (Doctoral dissertation). Universidade Federal do Rio Grande do Sul, Porto Alegre.
- Carvalho, N. O. (2008). *Hidrossedimentologia prática*. Rio de Janeiro: Interciência.
- Cohen, S., Kettner, A. J., Syvitski, J. P. M., & Fekete, B. M. (2013). WBMsed, a distributed global-scale riverine sediment flux model: model description and validation. *Computers & Geosciences*, 53, 80-93. <http://dx.doi.org/10.1016/j.cageo.2011.08.011>.
- Collischonn, W., Allasia, D., Silva, B. C., & Tucci, C. E. M. (2007). The MGB-IPH model for large-scale rainfall-runoff modelling. *Hydrological Sciences Journal*, 52(5), 878-895. <http://dx.doi.org/10.1623/hysj.52.5.878>.
- Dean, D. J., Topping, D. J., Schmidt, J. C., Griffiths, R. E., & Sabol, T. A. (2016). Sediment supply versus local hydraulic controls on sediment transport and storage in a river with large sediment loads. *Journal of Geophysical Research: Earth Surface*, 121, 82-110. <http://dx.doi.org/10.1002/2015JF003436>.
- Desmet, P. J. J., & Govers, G. (1996). A GIS procedure for automatically calculating the USLE LS factor on topographically complex landscape units. *Journal of Soil and Water Conservation*, 51(5), 427-433.

- Djebou, D. C. S. (2018). Assessment of sediment inflow to a reservoir using the SWAT model under undammed conditions: a case study for the Somerville reservoir, Texas, USA. *International Soil and Water Conservation Research*, 6(3), 222-229. <http://dx.doi.org/10.1016/j.iswcr.2018.03.003>.
- European Space Agency – ESA. (2018). *GlobCover*. Retrieved in 2022, December 12, from http://due.esrin.esa.int/page_globcover.php
- Fagundes, H. O., Fan, F. M., & Paiva, R. C. D. (2019). Automatic calibration of a large-scale sediment model using suspended sediment concentration, water quality, and remote sensing data. *Revista Brasileira de Recursos Hídricos*, 24, e26. <http://dx.doi.org/10.1590/2318-0331.241920180127>.
- Fagundes, H. O., Fan, F. M., Paiva, R. C. D., Siqueira, V. A., Buarque, D. C., Kornowski, L. W., Laipelt, L., & Collischonn, W. (2020a). Sediment flows in South America supported by daily hydrologic-hydrodynamic modeling. *ESS Open Archive*. Ahead of print. <https://doi.org/10.1002/essoar.10503046.2>.
- Fagundes, H. O., Paiva, R. C. D., Fan, F. M., Buarque, D. C., & Fassoni-Andrade, A. C. (2020b). Sediment modeling of a large-scale basin supported by remote sensing and in-situ observations. *Catena*, 190, 104535. <https://doi.org/10.1016/j.catena.2020.104535>.
- Fan, F. M., Buarque, D. C., Pontes, P. R. M., & Collischonn, W. (2015, November 22-27). Um mapa de Unidades de Resposta Hidrológica para a América do Sul. In Associação Brasileira de Recursos Hídricos (Org.), *XXI Simpósio Brasileiro de Recursos Hídricos* (pp. 1-8). Porto Alegre, Brazil: ABRH.
- Fan, F. M., Pontes, P. R. M., Buarque, D. C., & Collischonn, W. (2017). Evaluation of upper Uruguay river basin (Brazil) operational flood forecasts. *Revista Brasileira de Recursos Hídricos*, 22, e37. <http://dx.doi.org/10.1590/2318-0331.0217160027>.
- Fan, F., & Collischonn, W. (2014). Integração do modelo MGB-IPH com sistema de informação geográfica. *Revista Brasileira de Recursos Hídricos*, 19(1), 243-254. <http://dx.doi.org/10.21168/rbrh.v19n1.p243-254>.
- Farinasso, M., Carvalho, O. A., Guimarães, R. F., Gomes, R. A. T., & Ramos, V. M. (2006). Avaliação qualitativa do potencial de erosão laminar em grandes áreas por meio da EUPS - Equação Universal de Perdas de Solos utilizando novas metodologias em SIG para os cálculos dos seus fatores na região do Alto Parnaíba - PI - MA. *Revista Brasileira de Geomorfologia*, 7(2), 73-85.
- Farr, T. G., Rosen, P. A., Caro, E., Crippen, R., Duren, R., Hensley, S., Kobrick, M., Paller, M., Rodriguez, E., Roth, L., Seal, D., Shaffer, S., Shimada, J., Umland, J., Werner, M., Oskin, M., Burbank, D., & Alsdorf, D. (2007). The shuttle radar topography mission. *Reviews of Geophysics*, 45, 33.
- Flügel, W.-A. (1995). Delineating hydrological response units by geographical information system analyses for regional hydrological modelling using PRMS/MMS in the drainage basin of the River Bröl, Germany. *Hydrological Processes*, 9(3-4), 423-436. <http://dx.doi.org/10.1002/hyp.3360090313>.
- Föeger, L. B., Buarque, D. C., Pontes, P. R. M., Fagundes, H. O., & Fan, F. M. (2019, November 24-28). Modelagem hidrossedimentológica com propagação inercial de vazões. In Associação Brasileira de Recursos Hídricos (Org.), *XXIII Simpósio Brasileiro de Recursos Hídricos* (pp. 1-2). Porto Alegre, Brazil: ABRH.
- Franco, A. C. L., Oliveira, D. Y., & Bonumá, N. B. (2020). Comparison of single-site, multi-site and multi-variable SWAT calibration strategies. *Hydrological Sciences Journal*, 65(14), 2376-2389. <http://dx.doi.org/10.1080/02626667.2020.1810252>.
- Furl, C., Sharif, H., & Jeong, J. (2015). Analysis and simulation of large erosion events at central Texas unit source watersheds. *Journal of Hydrology*, 527, 494-504. <http://dx.doi.org/10.1016/j.jhydrol.2015.05.014>.
- Gupta, H. V., Kling, H., Yilmaz, K. K., & Martinez, G. F. (2009). Decomposition of the mean squared error and NSE performance criteria: implications for improving hydrological modelling. *Journal of Hydrology*, 377(1-2), 80-91. <http://dx.doi.org/10.1016/j.jhydrol.2009.08.003>.
- Hartmann, C., Bulla, L. A. S., & Fellini, B. D. (2010). Uso do ADCP na avaliação do fluxo e no transporte de sedimentos no baixo rio Jacuí, Charqueadas, RS/Brasil. *Gravel*, 8(1), 33-44.
- Instituto Brasileiro de Geografia e Estatística – IBGE. (1977). *Geografia do Brasil - região sul* (Vol. 5). Rio de Janeiro: IBGE.
- Instituto Brasileiro de Geografia e Estatística – IBGE. (2018). *Mapeamento dos recursos naturais do Brasil*. Retrieved in 2022, December 12, from geofp.ibge.gov.br/informacoes_ambientais/pedologia/vetores/escala_250_mil/
- Instituto Nacional de Tecnología Agropecuaria – INTA. (2013). *Suelos de la República Argentina*. Retrieved in 2022, December 12, from <http://www.geointa.inta.gob.ar/2013/05/26/suelos-de-la-republica-argentina/>
- Kaffas, K., & Hrisanthou, V. (2019). Computation of hourly sediment discharges and annual sediment yields by means of two soil erosion models in a mountainous basin. *International Journal of River Basin Management*, 17(1), 63-77. <http://dx.doi.org/10.1080/15715124.2017.1402777>.
- Kirchner, J. W. (2006). Getting the right answers for the right reasons: linking measurements, analyses, and models to advance the science of hydrology. *Water Resources Research*, 42(3), 1-5. <http://dx.doi.org/10.1029/2005WR004362>.
- Knoben, W. J. M., Freer, J. E., & Woods, R. A. (2019). Technical note: inherent benchmark or not? Comparing Nash-Sutcliffe and Kling-Gupta efficiency scores. *Hydrology and Earth System Sciences*, 23(10), 4323-4331. <http://dx.doi.org/10.5194/hess-23-4323-2019>.

- Koiter, A. J., Owens, P. N., Petticrew, E. L., & Lobb, D. A. (2013). The behavioural characteristics of sediment properties and their implications for sediment fingerprinting as an approach for identifying sediment sources in river basins. *Earth-Science Reviews*, *125*, 24-42. <http://dx.doi.org/10.1016/j.earscirev.2013.05.009>.
- Kumar, P. S., Praveen, T. V., Prasad, M. A., & Rao, P. S. (2018). Identification of critical erosion prone areas and computation of sediment yield using remote sensing and GIS: a case study on Sarada River Basin. *Journal of The Institution of Engineers: Series A*, *99*(4), 719-728. <https://doi.org/10.1007/s40030-018-0293-8>.
- Kumar, R., Samaniego, L., & Attinger, S. (2013). Implications of distributed hydrologic model parameterization on water fluxes at multiple scales and locations. *Water Resources Research*, *49*(1), 360-379. <http://dx.doi.org/10.1029/2012WR012195>.
- Lopes, V. A. R., Fan, F. M., Pontes, P. R. M., Siqueira, V. A., Collischonn, W., & Marques, D. M. (2018). A first integrated modelling of a river-lagoon large-scale hydrological system for forecasting purposes. *Journal of Hydrology*, *565*, 177-196. <http://dx.doi.org/10.1016/j.jhydrol.2018.08.011>.
- Maidment, D. (1993). *Handbook of hydrology*. New York, NY: McGraw-Hill Education.
- Merritt, W. S., Letcher, R. A., & Jakeman, A. J. (2003). A review of erosion and sediment transport models. *Environmental Modelling & Software*, *18*(8-9), 761-799. [http://dx.doi.org/10.1016/S1364-8152\(03\)00078-1](http://dx.doi.org/10.1016/S1364-8152(03)00078-1).
- Ministério do Meio Ambiente – MMA. (2006). *Caderno da região hidrográfica do Uruguai*. Brasília: Ministério do Meio Ambiente.
- Moriasi, D. N., Gitau, M. W., Pai, N., & Daggupati, P. (2015). Hydrologic and water quality models: performance measures and evaluation criteria. *Transactions of the ASABE*, *58*(6), 1763-1785. <http://dx.doi.org/10.13031/trans.58.10715>.
- Mueller, E. N., Güntner, A., Francke, T., & Mamede, G. (2010). Modelling sediment export, retention and reservoir sedimentation in drylands with the WASA-SED model. *Geoscientific Model Development*, *3*(1), 275-291. <http://dx.doi.org/10.5194/gmd-3-275-2010>.
- Paiva, R. C. D., Collischonn, W., & Tucci, C. E. M. (2011). Large scale hydrologic and hydrodynamic modeling using limited data and a GIS based approach. *Journal of Hydrology*, *406*(3-4), 170-181. <http://dx.doi.org/10.1016/j.jhydrol.2011.06.007>.
- Peters-Lidard, C. D., Clark, M., Samaniego, L., Verhoest, N. E. C., Van Emmerik, T., Uijlenhoet, R., Achieng, K., Franz, T. E., & Woods, R. (2017). Scaling, similarity, and the fourth paradigm for hydrology. *Hydrology and Earth System Sciences*, *21*(7), 3701-3713. <http://dx.doi.org/10.5194/hess-21-3701-2017>.
- Poblete, D., Arevalo, J., Nicolis, O., & Figueroa, F. (2020). Optimization of the Hydrologic Response Units (HRU) using gridded meteorological data and spatially varying parameters. *Water Resources Research*, *12*(12), 3558.
- Pontes, P. R. M., Fan, F. M., Fleischmann, A. S., Paiva, R. C. D., Buarque, D. C., Siqueira, V. A., Jardim, P. F., Sorribas, M. V., & Collischonn, W. (2017). MGB-IPH model for hydrological and hydraulic simulation of large floodplain river systems coupled with open source GIS. *Environmental Modelling & Software*, *94*, 1-20. <http://dx.doi.org/10.1016/j.envsoft.2017.03.029>.
- Qi, J., Li, S., Yang, Q., Xing, Z., & Meng, F. R. (2017). SWAT setup with long-term detailed landuse and management records and modification for a micro-watershed influenced by freeze-thaw cycles. *Water Resources Management*, *31*(12), 3953-3974. <http://dx.doi.org/10.1007/s11269-017-1718-2>.
- Rahmati, O., Tahmasebipour, N., Haghizadeh, A., Pourghasemi, H. R., & Feizizadeh, B. (2017). Evaluating the influence of geo-environmental factors on gully erosion in a semi-arid region of Iran: an integrated framework. *The Science of the Total Environment*, *579*, 913-927. <http://dx.doi.org/10.1016/j.scitotenv.2016.10.176>.
- Renard, K. G., Foster, G. R., Weesies, G. A., McCool, D. K., & Yoder, D. C. (1997). *Predicting soil erosion by water: a guide to conservation planning with the Revised Universal Soil Loss Equation (RUSLE)*. Washington, DC: U.S. Department of Agriculture. Agriculture handbook n°. 703.
- Rio Grande do Sul. Secretaria de Planejamento, Governança e Gestão – SEPLAG. (2019). *Atlas socioeconômico do Rio Grande do Sul* (4th ed.). Porto Alegre: SEPLAG. Retrieved in 2022, December 12, from <https://www.socioeconomicatlas.rs.gov.br/main-page>
- Rio Grande do Sul. Secretaria do Ambiente e Desenvolvimento Sustentável – SEMA. (2017). *Diagnóstico preliminar: descritivo dos eventos ocorridos no dia 5 de janeiro de 2017 entre as regiões dos municípios de São Francisco de Paula e Rolante/RS*. Porto Alegre: Secretaria do Ambiente e Desenvolvimento Sustentável.
- Rossoni, R. B., Fan, F. M., & Lopes, V. A. (2018, September 24-28). Estimativa da descarga sólida de sedimentos em suspensão para o Lago Guaíba/RS através da modelagem hidrossedimentológica de grande escala. In Associação Brasileira de Recursos Hídricos (Org.), *XIII Encontro Nacional de Engenharia de Sedimentos/ I Partículas nas Américas* (pp. 1-8). Porto Alegre, Brazil: ABRH.
- Sadeghi, S. H. R., Gholami, L., Darvishan, A. K., & Saeidi, P. (2014). A review of the application of the MUSLE model worldwide. *Hydrological Sciences Journal*, *59*(2), 365-375. <http://dx.doi.org/10.1080/02626667.2013.866239>.
- Samad, N., Chauhdry, M. H., Ashraf, M., Saleem, M., Hamid, Q., Babar, U., Tariq, H., & Farid, M. S. (2016). Sediment yield assessment and identification of check dam sites for Rawal Dam catchment. *Arabian Journal of Geosciences*, *9*(6), 466. <http://dx.doi.org/10.1007/s12517-016-2484-9>.

- Sari, V., dos Reis Castro, N. M., & Pedrollo, O. C. (2017). Estimate of Suspended Sediment Concentration from Monitored Data of Turbidity and Water Level Using Artificial Neural Networks. *Water Resources Management*, 31(15), 4909-4923. <http://dx.doi.org/10.1007/s11269-017-1785-4>.
- Sharpley, A. N., & Williams, J. R. (1990). *EPIC: The erosion-productivity impact calculator*. Washington, DC: U.S. Department of Agriculture. Technical bulletin n°. 1768.
- Silva, C. R., Chaves, H. M. L., & Camelo, A. P. (2011). Calibração e validação da equação universal de perda de solos modificada (MUSLE) utilizando dados hidrossedimentológicos locais. *Revista Brasileira de Ciência do Solo*, 35(4), 1431-1439. <http://dx.doi.org/10.1590/S0100-06832011000400037>.
- Silva, V. D. P. R., Silva, M. T., & Souza, E. P. (2016). Influence of land use change on sediment yield: a case study of the sub-middle of the São Francisco river basin. *Engenharia Agrícola*, 36(6), 1005-1015. <http://dx.doi.org/10.1590/1809-4430-eng.agric.v36n6p1005-1015/2016>.
- Tadesse, A., & Dai, W. (2019). Prediction of sedimentation in reservoirs by combining catchment based model and stream based model with limited data. *International Journal of Sediment Research*, 34(1), 27-37. <http://dx.doi.org/10.1016/j.ijsrc.2018.08.001>.
- Toldo Junior, E. E., Dillenburg, S. R., Corrêa, I. C. S., Almeida, L. E. S. B., Weschenfelder, J., & Gruber, N. L. S. (2006). Sedimentação de longo e curto período na Lagoa dos Patos, sul do Brasil. *Pesquisas em Geociências*, 33(2), 79-86. <http://dx.doi.org/10.22456/1807-9806.19516>.
- U.S. Department of Agriculture – USDA. *National engineering handbook*. Washington, DC: U.S. Department of Agriculture; 2009. Hydrologic soil groups. p. 1-13. Retrieved in 2022, December 12, from <https://directives.sc.egov.usda.gov/OpenNonWebContent.aspx?content=22526.wba>
- Vaz, A. C., Möller Junior, O. O., & Almeida, T. L. (2006). Análise quantitativa da descarga dos rios afluentes da Lagoa dos Patos. *Atlântica*, 28(1), 13-23. Retrieved in 2022, December 12, from <https://periodicos.furg.br/atlantica/article/view/1724/862>
- Vigiak, O., Malagó, A., Bouraoui, F., Vanmaercke, M., & Poesen, J. (2015). Adapting SWAT hillslope erosion model to predict sediment concentrations and yields in large Basins. *The Science of the Total Environment*, 538, 855-875. <http://dx.doi.org/10.1016/j.scitotenv.2015.08.095>.
- Vigiak, O., Malagó, A., Bouraoui, F., Vanmaercke, M., Obreja, F., Poesen, J., Habersack, H., Fehér, J., & Grošelj, S. (2017). Modelling sediment fluxes in the Danube River Basin with SWAT. *The Science of the Total Environment*, 599-600, 992-1012. <http://dx.doi.org/10.1016/j.scitotenv.2017.04.236>.
- Wang, J., Xu, K., Restrepo, G. A., Bentley, S. J., Meng, X., & Zhang, X. (2018). The coupling of bay hydrodynamics to sediment transport and its implication in micro-tidal wetland sustainability. *Marine Geology*, 405, 68-76. <http://dx.doi.org/10.1016/j.margeo.2018.08.005>.
- Wesselman, D., Winter, R., Oost, A., Hoekstra, P., & van der Vegt, M. (2019). The effect of washover geometry on sediment transport during inundation events. *Geomorphology*, 327, 28-47. <http://dx.doi.org/10.1016/j.geomorph.2018.10.014>.
- Williams, J. R. Sediment-yield prediction with universal equation using runoff energy factor. In: U.S. Department of Agriculture, organizer. *Present and prospective technology for predicting sediment yield and sources*. Washington, DC: U.S. Department of Agriculture; 1975. p. 244-252. Publication ARS-S-40.
- Wischmeier, W. H., & Smith, D. D. (1978). *Predicting rainfall erosion losses - a guide to conservation planning*. Washington, DC: U.S. Department of Agriculture. Agriculture handbook n° 537.
- Yapo, P. O., Gupta, H. V., & Sorooshian, S. (1998). Multi-objective global optimization for hydrologic models. *Journal of Hydrology*, 204(1-4), 83-97. [http://dx.doi.org/10.1016/S0022-1694\(97\)00107-8](http://dx.doi.org/10.1016/S0022-1694(97)00107-8).
- Zarzuelo, C., López-Ruiz, A., & Ortega-Sánchez, M. (2019). Evaluating the impact of dredging strategies at tidal inlets: performance assessment. *The Science of the Total Environment*, 658, 1069-1084. <http://dx.doi.org/10.1016/j.scitotenv.2018.12.227>.

Authors contributions

Renata Barão Rossoni: Conceptualization, Methodology, Software, Validation, Formal analysis, Investigation, Resources, Data Curation, Writing – Original Draft, Writing – Review and Editing, Visualization, Project administration.

Fernando Mainardi Fan: Conceptualization, Methodology, Software, Resources, Data Curation, Writing – Review and Editing, Supervision, Project administration, Funding acquisition.

Editor-in-Chief: Adilson Pinheiro

Associated Editor: Iran Lima Neto

SUPPLEMENTARY MATERIAL

Supplementary material accompanies this paper.

Table S1. Main studies related to the MUSLE equation, between 2015 to 2020

Figure S1. Soil Texture and Land Use and Cover map to South America. These maps were used as input information to development of HRUSed map. The soil texture map was based on Batjes (2005), IBGE (2018) and INTA (2013), land use and cover map was based on ESA (2018).

Figure S2. Comparison between HRUSed map and HRU map (Fan et al., 2015)

Table S2. Maximum, mean, and minimum values obtained for the hydrological model evaluation, for both maps for validation period (1990 to 1999)

Table S3. Performance metrics values obtained for HRU and HRUSed approaches for the calibration period (2000 to 2010) of SSC and SSD, calibrating with SSC and SSD. SD is Standard Deviation. Bold numbers indicate best result. Regional experiment.

Table S4. Statistic values obtained for hydrosedimentological model, for HRU and HRUSed approach (2000 to 2010). SD is Standard Deviation. Bold numbers indicate best result. Basin experiment.

Table S5. Statistic for KGE values obtained for hydrosedimentological model, for HRU and HRUSed (2000 to 2010). SD is Standard Deviation. Bold numbers indicate best result. Sub-basin experiment.

Figure S3. KGE values for SSD (2000 – 2010) calibration in the regional experiment. Calibrated with: (a) HRU and SSC, (b) HRUSed and SSC, (c) HRU and SSD, and (d) HRUSed and SSD. Limits between -0.41 to 1.

Figure S4. Spatialized KGE values for suspended sediment discharge (2000 – 2010) for basin experiment. (a) HRU, using SSC as parameter to calculate objective functions, (b) HRUSed, using SSC, (c) HRU, using SSD, and (d) HRUSed, using SSD. Values vary between -0.41 to 1 (best values)

Figure S5. Spatialized KGE values for suspended sediment discharge (2000 – 2010) for sub-basin . (a) HRU, using SSC as parameter to calculate objective functions, (b) HRUSed, using SSC, (c) HRU, using SSD, and (d) HRUSed, using SSD. Values vary between -0.41 to 1 (best values)

Figure S6. Validation results for hydrosedimentological modeling

This material is available as part of the online article from <https://doi.org/10.1590/2318-0331.282320220088>